SCIENCE CHINA
Chemistry

•REVIEWS•

June 2021 Vol.64 No.6: 879–898
https://doi.org/10.1007/s11426-021-9985-x

Interfacial compatibility issues in rechargeable solid-state lithium metal batteries: a review

Hongchun Wang[1], Jianping Zhu[2], Yu Su[2], Zhengliang Gong[1] & Yong Yang[1,2*]

[1]*College of Energy, Xiamen University, Xiamen 361102, China;*
[2]*Collaborative Innovation Center of Chemistry for Energy Materials, State Key Laboratory for Physical Chemistry of Solid Surface, College of Chemistry and Chemical Engineering, Xiamen University, Xiamen 361005, China*

Received January 09, 2021; accepted March 17, 2021; published online March 23, 2021

Solid-state lithium metal batteries (SSLBs) contain various kinds of interfaces, among which the solid electrode|solid electrolyte (ED|SE) interface plays a decisive role in the battery's power density and cycling stability. However, it is still lack of comprehensive knowledge and understanding about various interfacial physical/chemical processes so far. Although tremendous efforts have been dedicated to investigate the origin of large interfacial resistance and sluggish charge (electron/ion) transfer process, many scientific and technological challenges still remain to be clarified. In this review, we detach and discuss the critical individual challenge, including charge transfer process, chemical and electrochemical instability, space charge layers, physical contact and mechanical instability. The fundamental concepts, individual effects on the charge transfer and potential solutions are summarized based on material's thermodynamics, electrode kinetics and mechanical effects. It is anticipated that future research should focus on quantitative analysis, modeling analysis and *in-situ* microstructure characterizations in order to obtain an efficient manipulation about the complex interfacial behaviors in all solid-state Li batteries.

solid-state lithium metal batteries, interfacial compatibility, charge transfer kinetics, (electro-)chemical stability, space charge layer, mechanical stability

Citation: Wang H, Zhu J, Su Y, Gong Z, Yang Y. Interfacial compatibility issues in rechargeable solid-state lithium metal batteries: a review. *Sci China Chem*, 2021, 64: 879–898, https://doi.org/10.1007/s11426-021-9985-x

1 Introduction

Lithium-ion batteries are playing a more and more important role in our daily-life, ranging from consumer electronics and wearable devices to electric vehicles and energy storage station. The scenario demands advanced batteries with higher energy density and higher safety. Although lithium-ion batteries have made huge strides since their commercialization in 1990s [1,2], the development of traditional lithium-ion batteries has encountered a bottleneck nowadays. Besides, the energy density of present batteries cannot meet people's demand of high-mileage of electric vehicles, and fire accidents initiated by lithium-ion batteries are also frequently reported, which hinders their further rapid development. By replacing the liquid electrolytes with uninflammable inorganic solid electrolytes (SEs), safety concerns about thermal runaway and burning of organic electrolytes can be much relieved [3,4]. In spite of these advantages, solid-state batteries are still in infancy mainly because of these issues: poor processability and low ionic conductivity of most solid electrolytes, unstable solid|solid interface and corresponding high interfacial resistance. Enormous efforts have been devoted to developing highly conductive solid electrolytes by adjusting the composition or structure of materials [5]. Up to now, some sulfide electrolytes exhibit an ionic conductivity of 10^{-3} S cm^{-1} or even higher than liquid electrolytes. For example, $Li_{9.54}Si_{1.74}P_{1.44}S_{11.7}Cl_{0.3}$ has the highest reported ionic conductivity in all of the solid elec-

*Corresponding author (email: yyang@xmu.edu.cn)

trolytes [6]. The efforts on thinning the electrolyte layer have also brought down the bulk resistance of electrolytes to a low value [7]. Despite great progress in developing excellent lithium-ion conducting solid electrolytes, the rate capability of almost all cells is poor because of the large interfacial resistance and sluggish charge transfer (CT) evolved during charge/discharge cycles. Besides, the solid electrolytes and the heterogeneous junction interface could tolerate the volume changes of the electrode materials. Actually, the interfacial issue between solid electrolytes and electrodes, instead of the bulk conductivity, is playing an increasing role in the solid-state batteries' performances [8–15].

To develop advanced all solid-state lithium metal batteries (SSLBs), the solid electrode|solid electrolyte (ED|SE) interface should meet the following requirements: (1) excellent chemical and electrochemical stability against decomposition; (2) flexible or zero-strain design of the interface to avoid the electro-chemo-mechanical failure during cycling; (3) small interfacial impedance and fast charge transfer capability. The achievement of those criteria will facilitate the development and application of solid-state battery technology. However, the compatibility between the electrode materials and solid electrolytes is turning into the main technological blocking to the development of SSLBs, making the path to success far away.

Nevertheless, recent efforts have been devoted to helping uncover the nature of the complex interfacial behaviors. Main factors, such as chemical and electrochemical instability [12,16–20], space charge layers [21–23], poor physical contact and mechanical instability [24–28], are found to lead to the sluggish charge transfer kinetics at the interface. Even trickier, these factors are interrelated and difficult to be studied independently in a real solid system. A systematic discussion, especially from the basic sciences behind these individual issues, is still lacking, and the deep reasons why these factors will block the interfacial charge transfer process are often ambiguous and scattered, which relies on a comprehensive review summarizing the fundamental physicochemical concepts, available experimental results, and corresponding mathematical models to come forward to cast solution on these complex phenomena.

In this review, we overview the recent progress on the fundamental challenges at the electrode|electrolyte interface for understanding and solving the interfacial issues. Firstly, we highlight the importance of interfacial compatibility on cells' performances. Detailed discussions of each issue to illuminate the origin of the chemical/electrochemical/mechanical changes are provided, and corresponding solutions to address these interfacial issues are organized. Then, some promising advanced characterization techniques on probing the interfacial information are summarized, which is vital to help deepen our understanding about the real interface. Lastly, an outlook on theoretical models, experimental methods and present challenges is concluded as a guideline for future research.

2 Fundamental challenges at the electrode|electrolyte interfaces

To achieve long-range electric vehicles, high energy density electrode materials, such as lithium metal, nickel-rich materials, and high voltage materials, are necessary. However, these materials are highly chemical reactive with electrolytes. Preventing the chemical and electrochemical decomposition and extending the reduction/oxidation windows of solid electrolytes are therefore extensively discussed [8,29–31]. On the other hand, charge transfer process is mainly limited by the high-energy barrier and slow transfer kinetics at ED|SE interface [32–34]. The thermodynamically unstable nature of the two contact phases often results in the formation of solid electrolyte interphase (SEI) layers. The ionic conductivity of the layers is usually several orders of magnitude lower than that of bulk electrolyte materials, which acts as a high-energy barrier for the charge transfer process. Similar with that in the liquid system and semiconductors, space charge layers (SCLs) were also found at ED|SE interface in recent studies. Some researchers thought that the SCLs would introduce additional energy barrier for the ion transport across the accumulation/depletion region [23,35,36]. Hence, the sluggish transfer kinetics still remains as a huge challenge in a solid state battery system. In addition, the practically commercialized SSLBs need to experience thousands of cycles without obvious degradation, which raises huge challenges for the mechanical stability of interfaces. Since most electrode materials experience large volume changes during lithiation and delithiation, mechanical contact loss or cracking is unavoidable during the long cycling process [37,38]. Hence, how to compromise those stress-derived changes and keep enough charge transfer percolation networks requires the multidisciplinary integration, such as structure chemistry, interfacial engineering, mechanics, and computer sciences.

Figure 1 shows a schematic chart which summarizes the main fundamental challenges at electrode|solid electrolyte interfaces. In this section, we mainly describe some special issues. First, a mathematical description of the charge transfer resistance is discussed, and important factors blocking the interfacial kinetics will be identified. Later, different interfacial behaviors, in terms of chemical and electrochemical stability, the formation of interphase or interdiffusion layers, space charge layers, interfacial contact and mechanical stability, are discussed. We will focus on the physicochemical concepts and models for each factor and review the possible solutions to enhance the compatibility of the interfaces.

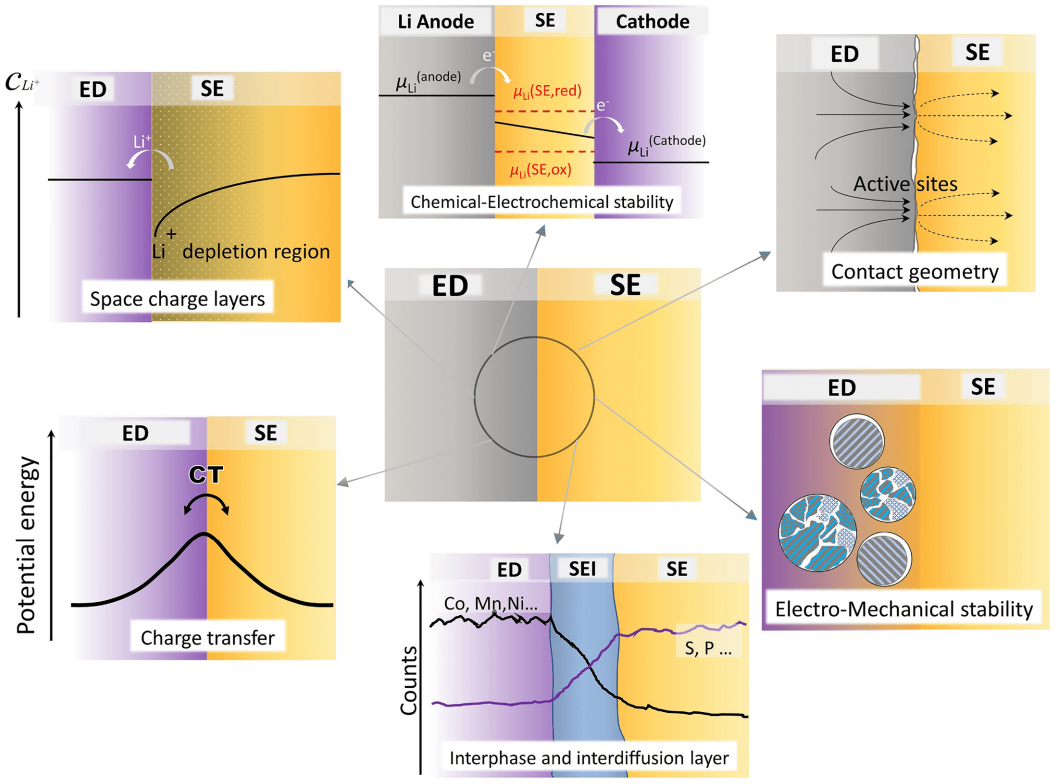

Figure 1 Main fundamental challenges at electrode|solid electrolyte interfaces (color online).

2.1 From liquid- to solid-state electrochemistry

Solid-state electrochemistry is a discipline which deals with the research on physical, chemical or electrochemical problems in the solid electrodes, solid electrolytes and their interfaces [39,40]. As an important branch of modern electrochemical sciences, solid-state electrochemistry follows the basic rules of electrochemistry and focuses on the electrochemical process inside the solid electrode, electrolytes and at the ED|SE interface.

There are many analogies between the conventional liquid-type electrochemistry and the solid-state electrochemistry. For example, both systems require the attention to the solid-state electrode reactions occurring at the interphases of the solid electrode|electrolytes. In addition, solid electrolytes enable us to build galvanic cells similar to those in liquids. In a liquid system, the charge transfer is achieved by dissociating solvated ions and further ion- and electron-transfer between electrodes and electrolytes. The solvated ions enable the conduction of the electric current in the liquid-type electrolytes. In solid electrolytes, the ionic conductivity is provided by the ionic transport (such as diffusion and electromigration) of charge carriers in solids. Such cells provide many new opportunities compared with liquid cells for scientific investigations and technical applications like batteries, sensors, and fuel cells. Hence, the general physical and chemical treatments of the galvanic cells with solid electrolytes are quite similar to that in the liquid system after considering the specific characteristics of the solids.

However, it is known that solid-state electrochemistry is quite different from the electrochemistry in liquid solutions. The large differences of physical, chemical and mechanical properties between liquids and solids have a strong impact on the electrochemical reaction process, mainly affecting interfacial transport and reaction kinetics. The first is the partial electronic conductivity [41]. SEs often show much higher partial electronic conductivity ($\sigma_e^{SE} \approx 10^{-8}$–$10^{-12}$ S cm^{-1}) [42] than liquid electrolytes (which can be considered as pure ionic conductors), which complicates local charge equilibrium and ion transport in SEs or at the interface. The second is the electrode reaction pathway. A general electrode reaction pathway in a liquid system includes (1) mass transfer, (2) electron transfer, (3) prepositive or subsequent chemical reactions (*i.e.*, protonation, dimerization or catalysis), and (4) surface reactions (*i.e.*, adsorption, desorption and crystallization) [40]. However, except for the necessary mass transfer and electron transfer steps, little is known about the other electrode reaction processes at solid-solid interfaces. Third, the interfacial structure and the electrochemical potential distribution of the solid electrode|solid electrolyte system are quite different from that of the liquid counterpart system. In liquid electrolytes, dipolar

solvent molecules and solvated ions play important roles in flexible screening interfacial potential drop near solid electrodes by high fluidity, while the solid framework is immobile or nearly-immobile in solid inorganic/polymer electrolytes. In addition, an important characteristic of solid-solid interfaces is that the local atomic structure can be significantly disordered and defective [43], or even hardly reproducible. This may greatly complicate the interfacial structure and interfacial charge equilibrium. Fourth, other factors, such as contact, stress, composition of the SEI, interfacial element diffusion, also show significant differences in two systems.

In general, solid-state electrochemistry and the conventional liquid-type electrochemistry theory are constructed on the same thermodynamic basis. However, due to the distinctive differences of solid electrolytes in physical, chemical and mechanical properties, we should be careful to analyze these new solid systems when we borrow some conclusions from the liquid-type electrochemical process.

2.2 Charge transfer kinetics

In a battery system, crossing the adjacent phase of the working Li ions or electrons is a complicated energy-consuming process and often causes large resistance. At electrode|solid electrolyte interfaces, charge transfer process is mainly controlled by the interfacial reaction kinetics. The resultant resistance, called charge transfer resistance (R_{ct}), has a negative effect on the battery performances. To figure out the main factors that affect the interfacial charge transfer resistance, the R_{ct} can be written as equation (1) according to Iriyama *et al*. [44] and Bard *et al*. [40].

At electrode|solid electrolyte interfaces in the charge transfer process,

$$R_{ct} = \frac{RT}{nFSi_0} \tag{1}$$

where R is gas constant, T is absolute temperature, n is the electron number of the charge transfer reaction, F is Faraday's constant, i_0 is exchange current density and S is the electrode area (electrochemical active sites). Here, the exchange current density (i_0) is a crucial parameter describing the interface kinetics and can be written as

$$i_0 = nFk^0\left(c_{ED}^*\right)^{1-\alpha}\left(c_{SE}^*\right)^{\alpha} \tag{2}$$

where k^0 is standard rate constant, α is transfer coefficient, c_{ED}^* is lithium concentration in the electrode, and c_{SE}^* is lithium concentration in the solid electrolyte. Based on the absolute rate theory (transition state theory), the k^0 is a function of frequency factor (B) and activation energy (E_a) and can be described as follows:

$$k^0 = B\exp\left(-\frac{E_a}{RT}\right) \tag{3}$$

By assembling the equations (1−3), the given equation is derived as follows:

$$\frac{T}{R_{ct}} = \frac{n^2F^2}{R}BS\left(c_{ED}^*\right)^{1-\alpha}\left(c_{SE}^*\right)^{\alpha}\exp\left(-\frac{E_a}{RT}\right) \tag{4}$$

Here, by substituting the pre-exponential part as A, the simplified equation can be written as:

$$\frac{T}{R_{ct}} = A\exp\left(\frac{E_a}{RT}\right) \tag{5}$$

It should be noted that the above equations are based on a simplified Butler-Volmer model, which is derived from electronic charge transfer process under the diluted solution approximation. The real situation can be much more complicated because of the totally different properties of solid electrolytes. Nevertheless, these equations provide valuable references to obtain a better understanding on the origin of the high charge transfer resistance. From the above formula, we can identify important parameters that affect charge transfer process and speculate on the possible causes that hinder the fast transfer kinetics in a realistic solid-state battery system. Parameters that can cause significant resistance variation are E_a, S, T, c_{ED}^* and c_{SE}^*.

Based on the transition state theory [51] and above equations, the smaller charge-transfer activation energy is, the faster the dynamics and larger the exchange current is. E_a can be estimated from the temperature-dependent charge transfer resistance at interfaces. Table 1 summarizes the apparent activation energy of charge transfer reactions for various kinds of interfaces. It is interesting that the obtained apparent E_a for interfacial charge-transfer reactions is almost close to that for ionic conduction in solid electrolytes, which means that the charge transfer process at ED|SE interfaces also plays a decisive role in solid-state systems. Besides, since the real interface is often thermodynamically unfavorable (which will be discussed later), and the formed interphase is composed of at least two different nano-phases which typically have a low ionic conductivity [52–54]. In this situation, a larger activation energy for charge transfer generated at the interface with higher energy barrier during the formation of interfaces between electrode|electrolytes [50]. Hence, a more rigorous study should consider the existing microscopic charge transfer processes: (1) interfaces between electrodes and the SEI layer, (2) the transportation within the SEI, and (3) the charge transfer between SEI and solid electrolytes [55]. Such a SEI layer will undoubtedly complicate the charge transfer process and lead to a larger energy barrier. Figure 2 schematically presents the charge transfer processes of three electrode|electrolyte interfaces with/without formed SEI layers.

On the other hand, S is related to the electrochemical active sites for charge transfer reactions. Poor physical/chemical contacts between active materials and electrolytes seriously restrict the percolation pathways for charge transfer. Hence,

Table 1 Survey of activation energy (E_a) for charge transfer reactions at electrode|solid electrolyte interfaces

Solid electrolyte (SE)	E_a of SE (kJ mol^{-1})	Electrode (ED)	E_a of charge transfer reaction (kJ mol^{-1})	References
LiPON	58	$LiCoO_2$	57	[45]
LLTO	30	$LiMn_2O_4$	38	[46]
LLZO	30	$LiCoO_2$	30	[47]
LLZO	30	Li	30	[47]
$Li_7La_3Zr_2O_{12}$ (28 mol% Al)	34.72	Li	39.54	[48]
$Li_{6.625}La_3Zr_{1.625}Ta_{0.375}O_{12}$ (29 mol% Al)	39.58	Li	42.43	[48]
$Li_6La_3ZrTaO_{12}$	44.36	Li	44.36	[48]
LLZO	32.79 (Bulk)	Li	35.68	[49]
LLZO	41.46 (Grain boundary)	Li	35.68	[49]
Li_6PS_5Br	10.13	Micro Li_2S	/	[50]
Li_6PS_5Br	10.13	Nano-Li_2S	/	[50]
Li_6PS_5Br	10.13	Mixed nano-Li_2S	12.54	[50]
Li_6PS_5Br	10.13	Annealed mixed nano-Li_2S	9.64	[50]
Li_6PS_5Br	10.13	Mixed nano-Li_2S (cycled)	37.61	[50]
LAGP	/	LiV_2O_5	30.37	[23]
LAGP	/	$Li_2V_2O_5$	49.67	[23]

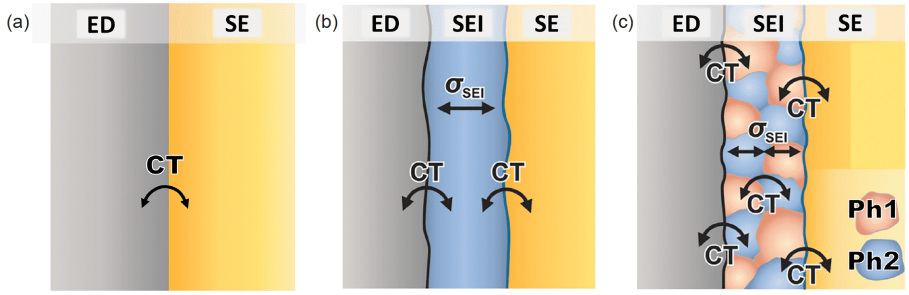

Figure 2 Schematic charge transfer processes at electrode|electrolyte interfaces: (a) Thermodynamically stable interface, where no interphase is formed; (b) Homogeneous single-phase SEI is formed; (c) Multiphase SEI is formed. In case a, only one CT process exists. In case b, two different CT processes exist, which are totally different from ideal CT process in case a. In case c, more CT processes appear depending on the number of components in SEI [55] (color online).

large interface activation energy is expected at solid|solid interfaces. In fact, extensive studies have been carried out to improve the original contact geometry in recent years [56–60]. Another fundamental problem is the electro-mechanical contact loss during cycling [24,61]. Large volumetric change of active materials will lead to mechanical detachment of original interfaces and the active sites for charge transfer will be substantially reduced. It is now a big rising challenge to maintain high utilization of active materials and keep less loss of active lithium in solid state batteries. As for c_{ED}^* and c_{SE}^*, the lithium concentration can be very different, depending on the applied voltages. The formation of interphases and space charge phenomena can also significantly change local carrier concentration. Other factors, such as temperature and contaminants, can also affect local ion distribution but they are not the focus of this review. In general, the interphase, space charge phenomena, contact geometry and state of charge (SOC) will greatly influence the charge transfer processes, which requires a thorough understanding of those basic concepts to promote the interfacial kinetics.

2.3 Chemical and electrochemical stability of the interfaces

2.3.1 Electrochemical stability window

The stability of SE paired with high energy-density cathodes/anodes is the most important parameter right now in the design of state-of-the-art SSLBs, which requires a stable and reliable interface from both chemical and electrochemical points. In a battery system, an ideal interface needs to be both thermodynamically stable and kinetically stable (or at least kinetically stable) under the open circuit or steady-state

current condition, so it is necessary to understand the interface in terms of thermodynamics and dynamics. Concretely, we need to consider the following questions for a practical interface: (1) can solid electrolytes resist the decomposition under different applied voltages? (2) Is SE chemically stable upon the contact with electrode materials? (3) How is the electrochemical stability of the contact interface during cycling [62], and (4) whether the interfacial (electro-)chemical reaction is kinetically self-limiting with/without applied current?

In general, the ED|SE interfacial stability is governed by the electrochemical stability window (ESW) of the used electrolyte, which is determined by its composition and structure. There are two commonly accepted theories to estimate the electrochemical stability of the SE, "band gap approach" and "phase stability method", as summarized by Janek *et al*. [55] (Figure 3(a, b)), both of which originate from thermodynamic stability estimation.

Solid electrolytes can be regarded as a pure ionic conductor with negligible electronic conductivity, and the electrode materials are typically semiconductors. Hence, the ED|SE interfacial behaviors can be explained by semiconductor physics with their relative gap states [21]. According to the "band gap approach", the ESW of SE is described by its conduction band minimum (CBM) and valence band maximum (VBM), and the interface stability is mainly controlled by the relative electron level of the two contact phases. At the anode side, electrons will be transferred from the electrode to the empty electron orbit (CBM) of electrolytes if the electron energy of electrodes is high enough, which is common when alkali metal anodes, *i.e.*, lithium metal, are used or a more negative potential is reached. The electrolyte will be reduced in such situation. On the cathode side, in a similar way, because of the low Li chemical potential of active materials, electrons are more likely to be transferred to the electrode. When the VBM of SE is above the CBM level of electrodes, the electrolyte is oxidized. The band gap estimation gives an intuitive way to understand the interface stability from the energy level. However, this method is under the assumption that there is no interfacial diffusion and chemical reactions between the contact components. Hence, it only provides an approximate value and cannot obtain the exact decomposition potential [64].

Another method to estimate the ESW of solid electrolytes is the phase stability method originating from the thermodynamic analysis based on the first-principles calculations and strictly yields the correct thermodynamic stability potentials [30,62,65]. With this method, the phase equilibrium combinations with the lowest Gibbs free energy at different potentials can be measured. If a reaction is thermodynamically favorable at a given potential, the electrolyte will undergo a reduction/oxidation reaction with electrode materials and produce a low-energy phase equilibrium composition. By screening the most favorable reaction at

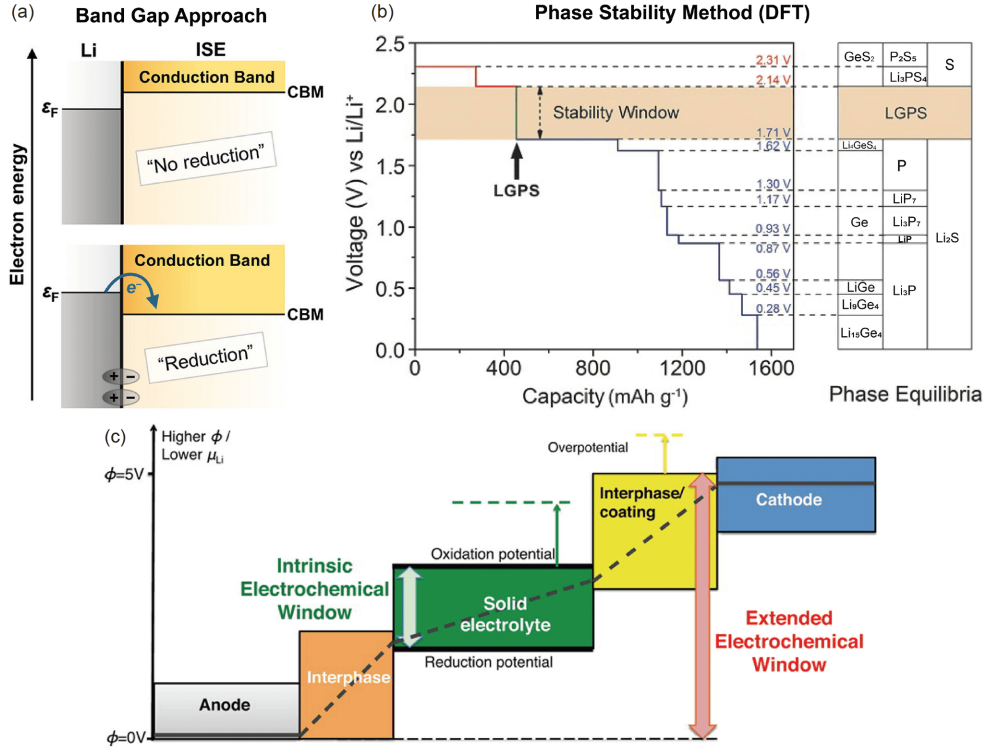

Figure 3 (a) Electrochemical stability of an SE in contact with lithium metal anodes according to the simplified "band gap approach" [55]. (b) Thermodynamic potential windows for a $Li_{10}GeP_2S_{12}$ (LGPS) SE evaluated by the "phase stability method" [29]. (c) Schematic illustration of the extended electrochemical stability by interphase and coating [63] (color online).

different potentials, we can obtain the ESW of the solid electrolyte materials at different SOC and corresponding reaction products. Indeed, the phase stability method provides a lower limit of ESW as it assumes full thermodynamic equilibrium and neglects the kinetic limitation in the reaction and transportation.

The kinetic limitation could be far more important since the decomposition of SEs is thermodynamically favorable in most of the scenario. Although accurate dynamical estimation for interfacial stability based on theoretical researches are seldom reported, we can glean some information from the existing experiment results. Early experimental measurements of the electrochemical stability window showed that solid electrolytes have larger ESW. For example, tests based on a Li|SE|semi-blocking electrode reported a very wide ESW for both $Li_{10}GeP_2S_{12}$ (LGPS) and $Li_7La_3Zr_2O_{12}$ (LLZO) [66,67]. However, the assembled solid-state batteries often suffer fast degradation. Wang *et al*. [29] found the limited contact area of electrodes and electrolytes will restrict the electron transfer, and thus enlarged the measured ESW. These results indicate that interfacial electron transport governs the decomposition reaction kinetics of solid electrolytes. On the other hand, if SE suffers mild (electro-) chemical reactions with electrodes at the interfacial region, where a SEI with low ionic resistance and low electronic conductivity as well as limited thickness can be formed, and then the ED|SE interface is considered to be kinetically stable. For example, $LiZr_2(PO_4)_3$ and $Li_{1.5}Al_{0.5}Ge_{1.5}(PO_4)_3$ possess the same rhombohedral structure. However $LiZr_2(PO_4)_3$ is reported to be stable with lithium while $Li_{1.5}Al_{0.5}Ge_{1.5}(PO_4)_3$ suffers severe side reactions with lithium metal anodes. The reason is that $LiZr_2(PO_4)_3$ can mildly react with lithium to form a thin passivation SEI layer composed of Li_3P and Li_8ZrO_6 with ion transport capability [68]. For $Li_{1.5}Al_{0.5}Ge_{1.5}(PO_4)_3$, the Ge^{4+} can be directly reduced to Ge metal state and form Li–Ge alloy with high electronic conductivity [69]. Wenzel *et al*. [70] combined *in-situ* X-ray photoelectron spectroscopy (XPS) technique and time-resolved impedance spectroscopy to investigate the stability and interphase growth of $Li_{10}GeP_2S_{12}$ and $Li_7P_3S_{11}$ in contact with Li metal anodes. The parabolic dependence between SEI thickness and time suggests that a diffusion-controlled growth mechanism exist at the interface. The parabolic growth constant of $(2.33\pm0.22)\times10^{-8}$ cm $h^{-0.5}$ for $Li_7P_3S_{11}$ is much smaller than that of $(3.60\pm0.08)\times10^{-7}$ cm $h^{-0.5}$ for LGPS. This result demonstrates that LPS shows the slower interphase growth and smaller total SEI resistance for its "mild" reduction reaction with Li metal than LGPS, and appears to be a more favorable material for the applications in lithium-metal-containing SSLBs.

2.3.2 *Interphase or mutual diffusion layer*

For a thermodynamically stable battery, the chemical potential of cathodes (μ_C) and anodes (μ_A) should be located within the ESW of the electrolyte. However, this situation is extremely rare among the known solid electrolytes. The formation of interphases or element mutual diffusion layers is unavoidable because of the large thermodynamical driving force. Hence, most of electrolytes suffer from serious interfacial degradation and erosion. This is one of the most important sources of the growing interfacial impedance observed experimentally. Therefore, the characteristics of interphase and transport kinetics of the carriers through these interphases play an extremely important role in the overall performances of SSLBs. Considering the interfacial stability from the point of view of interphase properties, several aspects need be taken into consideration according to the experimental results and theoretical analysis: (1) what is the thermodynamic and kinetic nature of interfacial stability? (2) Which type of interface/interphase is kinetically self-limiting? (3) How is constructed a kinetically stable interface or a buffer layer? To answer these questions, our first priority is to distinguish the types of the interfaces. Wenzel *et al*. [71] classified the ED|SE interfaces into three different categories based on their thermodynamic and kinetic characteristics: (1) an ideal, nonreactive ED|SE interface, which is thermodynamically stable; (2) a reactive and evolutionary interface, where a mixed-ionic/electronic conducting interphase (MCI) forms and the interfacial reaction is both thermodynamically and kinetically favorable; (3) a self-limiting metastable interface, where an almost electrical insulating, stable SEI forms and the interfacial reaction is thermodynamically favorable but kinetically limited.

Actually, there is almost no absolutely thermodynamic stable interface, as described in (1). Both calculated and experimental results indicate that most of solid electrolytes have a narrow ESW. Among the reported solid electrolytes with high ionic conductivity, Li cubic-garnet (LLZO) shows extremely high stability with Li metal because of its low equilibrium potential (0.05 V *vs*. Li/Li^+) [29], and the thermodynamic driving force for reduction is negligible. For the thermodynamically unstable interface (2) and (3), both of them are MCI-type interphase in principle. The main difference is their ability to insulate electrons. If electrons keep transport across the interphase, continuous reduction of electrolytes will happen. Hence, the partial electron conductivity of the interphase should be as low as possible in order to form a kinetically stable SEI layer rather than a MCI layer, and this principle is also applied to coating layers which we will discuss in detail next. As a representative of interfacial stability research, a sulfides|Li metal interface has been extensively investigated. Most sulfide electrolytes are sensitive to Li metal electrodes for their relatively high thermodynamic reduction potential ~1.7 V [62]. Both MCI-type and SEI-type interphase will be formed, depending on the used electrolytes. In contact to Li metal, the $Li_{10}GeP_2S_{12}$/

$Li_{10}SnP_2S_{12}$ electrolytes will be reduced to Ge^0/Sn^0, Li–Ge/Li–Sn alloy, which are high electronic conductivity phases and will further accelerate the decomposition reaction, *i.e.*, MCI-type interphase. By using Li_6PS_5Cl or Li_3PS_4 as electrolytes, the produced interphases are mainly composed of Li_2S, Li_3P and LiCl, whose electronic conductivity are low, and are therefore SEI-type. Indeed, the SSLBs with these SEs show good compatibility with Li metal anodes. Generally speaking, the electrolytes containing variable valence metal cations, such as Ti^{4+}, Ge^{4+}, Sn^{4+}, are more likely to form MCI mesophase at anode interfaces.

The mutual element diffusion between two phases is also a serious challenge at ED|SE interfaces. Sakuda *et al*. [72] first observed the diffusion of cobalt from charged $LiCoO_2$ (LCO) cathodes to the sulfide electrolyte by high-angle annular dark-field scanning transmission electron microscopy (HAADF-STEM) and energy dispersive x-ray spectroscopy (EDX). Later, computational results also confirmed that the Co↔P cation exchange at the LCO|sulfide interface is energetically preferable [52,73]. The consequently formed interdiffusion layer is MCI-type with high electronic conductive species (*e.g.*, CoS), which drives continuous degradation of the interface and ultimately leads to large interfacial resistance and poor cycle life. Woo *et al*. [74] analyzed the interface between $LiCoO_2$ and $Li_{3.15}Ge_{0.15}P_{0.85}S_4$ SE. The TEM-EDS line profiles show a region where Co, S, and P coexist, which is attributed to the formation of mutual diffusion interfacial layers. Further analysis shows the diffusion depth of Co is estimated to be approximately 30 nm. Sakuda *et al*. [72] observed the ED|SE interface between $LiCoO_2$ electrodes and Li_2S–P_2S_5 solid electrolytes after the initial charging. TEM observations suggest that mutual diffusion of elements occurred. The Co element is observed even at a distance of 50 nm from the interface. On the other hand, high-temperature thermal treatment is a prevailing method to achieve an intimate contact between cathodes and oxide SEs. However, it will introduce a mutual diffusion layer with high resistance because of the enhanced dynamics at high temperature. Park *et al*. [75] found that there were inevitable interactions during the co-sintering process to fuse LCO and LLZO. The cubic LLZO surface was partially transformed into the tetragonal phase because of the migration of Al. Another special case comes from solid polymer electrolyte (SPE) batteries, which is known for their excellent mechanical compatibility with electrodes. Song *et al*. [76] monitored the interface evolution of the working S|SPE|Li batteries by *in-situ* optical microscope (OM) imaging. An irreversible color transformation in the polymer-ceramic composite electrolyte was directly captured during cycling, and the XPS and Raman analysis confirmed the accumulation of polysulfides on the metallic lithium anode, which indicated a shuttling process of polysulfides in solid-state polymer electrolytes. These examples provide a deep insight into the diffusions of elements in a working SSLB.

2.3.3 Solutions to the interfacial chemical and electrochemical instability

To alleviate the undesirable interfacial reactions between electrodes and solid electrolyte materials, several effective strategies have been developed to mitigate the key issues associated with chemical and electrochemical instability. The solutions can be divided into the following three main aspects: (1) anode|SE interface regulation. First of all, selecting suitable electrode materials with the working voltage within the ESW of solid electrolytes is a simple and thermodynamically feasible method. For example, the decomposition will be avoided if $Li_4Ti_5O_{12}$ (LTO, ~1.5 V *vs*. Li/Li^+) anodes are paired with sulfide electrolytes [77]. However, these materials significantly decrease the energy density of SSLBs. Secondly, replacing the pure Li metal anode by lithium alloy, such as Li–Al, Li–Sn, and Li–In, can reduce lithium chemical potential change at interfaces and protect SE against decomposition. Li–In alloy(~0.6 V *vs*. Li/Li^+) demonstrated superior performances with LGPS electrolytes compared to Li metal because of its higher equilibrium potential to suppress the reduction of electrolytes [29]. In addition, interfacial kinetic regulation, such as surface passivation treatment, buffer layer and special design for interfacial structures or electrode materials, is also widely adopted. Liang *et al*. [78] reported that the Li_3PS_4|Li interface can be stabilized by an *in-situ* formed Li_xSiS_y protection layer, which is electronically insulating and can block the side reaction between Li and sulfide electrolytes. Recently, Samsung Advanced Institute of Technology [79] reported a nano-size Ag–C composite anode, which can effectively regulate Li deposition away from the solid electrolyte|anode interface and then enhance the interfacial stability. Although the exact mechanism regulating the Li deposition sites on the current collector instead of composite anodes|SE interfaces remains unknown, it provides a new way of thinking and perspective for solving interface stability problems. (2) Cathode|SE interface regulation. Artificial coatings and buffer layers (Figure 3(c)) are the mostly used modification method and are found to improve the charging-discharging performance of several cathode|SE interfaces. From the physicochemical point of view, the coatings/buffer layers have three mechanisms of action. (1) Blocking the interfacial electron transport by the coated electronic insulating layer, which provides a kinetically stable interface. (2) Tuning the ESW mismatch of the contact with SE and ED by applied proper coating materials with a large bandgap. In particular, d^0 oxides, such as $LiNbO_3$ (LNO) and $Li_4Ti_5O_{12}$, have lower VBMs [21], and this provides a thermodynamic stable method. For example, $LiNbO_3$ is found effectively preventing the oxidation of electrolytes at high applied voltages and significantly reducing the interfacial resistance, because of

the wide ESW of $LiNbO_3$ that can compromise the mismatch of electronic energy levels between two phases [80]. (3) Eliminating the cross-diffusions of elements. The artificial coating layers, such as $Li_4Ti_5O_{12}$ [81] and Li_3BO_3 (LBO) [75], have been applied at cathode material|SE interface to suppress the interfacial mutual diffusion phenomena. These examples show that the coating layer can stabilize the ED|SE interface thermodynamically and kinetically. It should be noted that as an extension of atomic layer deposition (ALD), molecular layer deposition (MLD) technology can provide precise and uniform deposition of organics and inorganic-organic hybrid materials for interfacial engineering, and will attract more attention in the future [82]. Except that, the emerging sintering techniques bring additional benefit for solid oxide electrolyte|cathode interfaces. As we have mentioned above, high temperature treatment is necessary to enhance the contact of this type of interfaces, but parasitic reactions are inevitable. As the interfacial reactions are also controlled by thermal dynamics, reducing the reaction time and lowering the reaction temperature can inhibit interfacial side reactions to some extent. Recent years, field-assisted sintering techniques (FAST) [83,84], such as spark plasma sintering (SPS), hot-pressed sintering (HPS), have been successfully proven as a fast means of fusing cathode materials and oxide SEs. The faster processing with high heating and cooling rate, shorter dwell time and, especially, lower sintering temperature may minimize the formation of secondary phase and decrease mutual diffusion. (3) Extending the electrochemical stability window of electrolytes. It is difficult for one electrolyte to possess both high oxidation stability and reduction stability. To combine the preponderances of different electrolytes, multiple-layer electrolyte configuration has been put forward to achieve both cathodic and anodic interface stability. A $75Li_2S$-$24P_2S_5$-P_2O_5 electrolyte layer, which was stable against Li metal anodes, was introduced into Li|LGPS interfaces to extend the cut-off voltage of batteries by Yao *et al*. [85]. Similarly, Guo *et al*. [86] extended the electrochemical window of solid polymer electrolytes to 0–5 V *via* heterogeneous multilayered structures for high-voltage lithium metal batteries. Some recently discovered halide electrolytes, such as Li_3ScCl_3, possess excellent air stability, high ionic conductivity and, especially, high oxidation stability [87]. As most of sulfide electrolytes are intolerant to oxidation and incompatible with oxide cathode materials, the introduction of halide electrolytes in the cathode side will help to solve stability issues. In this way, the halide electrolytes deserve more attention in the future [88]. Expanding the intrinsic stability window of electrolytes is another feasible way. More recently, Zhang *et al.* [89] showed that substituting the tetrahedra PS_4 with PO_4 and maintaining the composition of the original GeS_4 in $Li_{14}P_2Ge_2S_{16}$ to form $Li_{14}P_2Ge_2S_8O_8$ will improve the oxidative stability (from 2.3 to 2.89 V). This work provides potential strategy to extend the ESW of SEs through compositional tuning.

2.4 Space charge layer

2.4.1 Space charge phenomena

Substantial studies have focused on chemical and electrochemical stability of electrode|electrolyte interfaces, and the interphases or interdiffusion layers indeed take a great contribution to the slow charge transfer process in SSLBs. By contrast, less attention is paid to the space charge phenomena at ED|SE interfaces, but there are growing evidences indicating the importance of SCL on the battery performances [23,35,90]. A fundamental understanding, both experimentally and theoretically, is still unsatisfactory until now. In general, the two contact phases have different chemical potentials, which provides a driving force to redistribute charges within the interface core zone to lower the overall energy, leading to one charge enriching on the one side of the core while the other side compensated by an equal but opposite charge, thus developing a space zone of carrier accumulation/depletion at interfaces, called space charge layer [12,32,91]. It is believed that the SCL will bring additional energy barriers for charge transfer by introducing a large concentration and electric gradient field in this region.

In conventional liquid-based ion batteries, the accumulated surface charge and interfacial potential drop can be screened by the dipole changes of solvent molecules and ion concentration polarization. The distribution of the mobile cations and anions near the surface of ED in the electrolyte can be described by the Gouy-Chapman mode, called electric double layer (EDL), which contains a Helmholtz layer and a diffusion layer, and the typical width of EDL is in the order of the Debye length (~1–10 nm) [21]. By using solid electrolytes, the charge and potential screening can only be achieved by the accumulation or depletion of charge carriers such as ions and vacancies, because of the immovability of anion frameworks (except for solid polymer electrolytes), thus leading to the formation of SCL [33]. However, the fundament of SCL theories at a solid|solid interface is rarely studied. Some questions still need to be clarified. For example, is there a distinction between a tight layer and a diffused layer as that in a liquid system? Is there a generalized model to describe interface carrier change? Why the reported widths are significantly large? And most importantly, what kind of role SCL plays in the battery performances?

2.4.2 Measurements of SCL and its effects

Observation on space charge phenomena is a great challenge, and the predominant reason is the limited experimental method directly access to ionic concentration and energy levels and also to their electronic counterparts at the core

zone. Otherwise, the selection of experimental systems, preparation of samples and equipment performances are also very important. Yamamoto *et al.* [92] used quantitative electron holography (EH) to dynamically monitor the potential profile and its distribution across the LCO|SE interface, as shown in Figure 4(a). The line profiles clearly displayed a steep potential drop at the interface followed with a gradual slope in the electrolyte zone, which provides a direct evidence for the formation of SCL due to Li^+ accumulation/deletion during cycling. Fingerle *et al.* [93] investigated $LiCoO_2$|LiPON interface with XPS. The mapped energy level diagram indicated the presence of a space charge layer, which was related to the chemical potential differences between the two contact materials. Except for experimental studies, modeling on space charge layer is an important approach to gain a better understanding of its nature and effects. Developed models can not only provide plenty of information, such as lithium concentration distribution, potentials profiles, chemical potential changes, corresponding electronic states and thickness, but also the effects of related factors on space charge layers. Braun *et al.* [36] derived a thermodynamically consistent mathematical model for SCL formation in a solid electrolyte based on first-principle calculations. The semi-analytical solution showed that the width of developed space-charge region highly depended on the dielectric properties of the electrolyte materials, while other factors, such as external potential difference or the mixing behavior, only played a minor role. The elements mutual diffusion also affected interfacial Li ion rearrangement. Tateyama *et al.* [21] combined the density functional theory (DFT)+U calculations and nudged elastic band techniques to investigate the interface. They pointed out that there existed a dynamic growth process of Li^+ depletion layers during charging, and interfacial reactions accompanied with Co↔P exchange could enhance this effect although the exchanged structure had few geometrical bottlenecks, which could be taken as a microscopic origin of the interfacial resistance.

The role of SCL on the charge transfer at ED|SE interfaces is still in debate. Some researchers thought that the relations between the high interfacial impedance and SCLs were largely overestimated, especially for the Li|SEs interface [55]. Recently, Klerk *et al.* [90] presented a space charge model with consideration of coulombic interactions between the defects within space charge regions. The predictions demonstrated that the SCL was only about a few nanometers in thickness and the assessed interfacial capacitance and resistance was negligibly small (Figure 4(b)). Otherwise, the reported low CT resistances for Li|SEs interfaces also suggested that SCL was not mainly responsible for the limited interface kinetics. Others emphasized the importance of this effect, which would lead to a higher barrier for Li-ion diffusion and smaller exchange current density and thus a significantly higher interface resistance. Swift *et al.* [22] presented a fully first-principle-informed model to build the potential profiles in a Li|LiPON|Li_xCoO_2 battery. Their work revealed that the anode interface always played a blocking role in the discharging, while the LiPON|cathode interface potential drop would reduce the discharge barrier at high SOC and increase it at low SOC (Figure 4(c)). These results

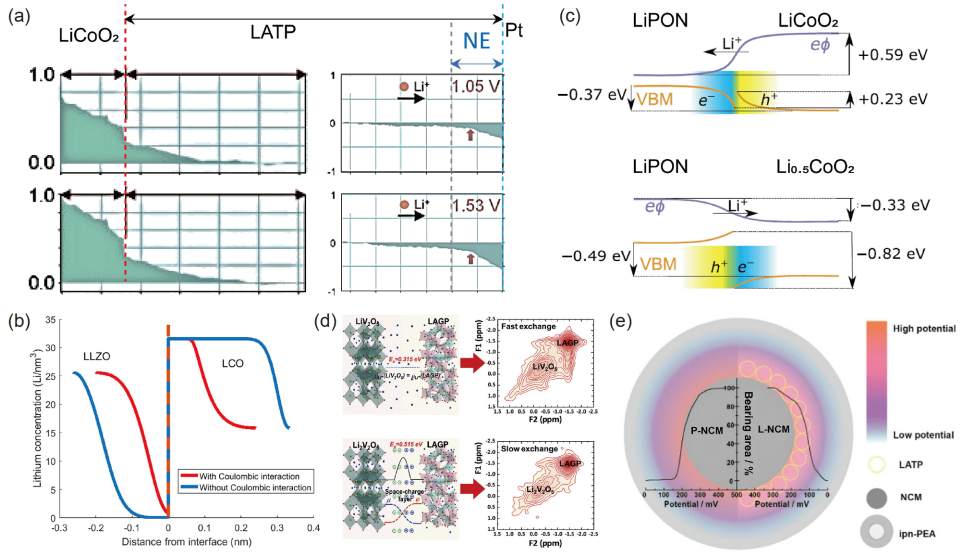

Figure 4 (a) Voltage profiles around $LiCoO_2$|LATP interface (left) and LATP|Pt interface (right) measured by electron holography at different charging voltages. NE is the *in-situ* formed negative electrode material, scale length: μm [92,94]. (b) Lithium concentration at the LCO|LLZO interface at 4.3 V with and without Coulomb interactions [90]. (c) Schematic of the electrostatic potential and valence bands at the LiPON and Li_xCoO_2 interfaces [22]. (d) Schematic representation of the impact of the space-charge layer at the interface of LiV_2O_5|LAGP and $Li_2V_2O_5$|LAGP and corresponding ^{6}Li NMR exchange experiments [23]. (e) Schematic diagram with bearing analysis and potential distribution of the P–NCM and L–NCM (with LATP modified) cathodes [95] (color online).

Table 2 Summary of the recent representative researches on interfacial space charge layers

Electrode|solid electrolyte (Coating)	Methods	Main conclusions	Reference
LCO|LATSP|Pt	Quantitative electron holography (EH) +electron energy loss spectroscopy (EELS)	An electric double layer forms at the interface as a result of lithium-ion accumulation/depletion	[92,94]
LCO|LiPON (LNO)	XPS+electrochemical techniques	Chemical coordination near the interface providing experimental validation of space-charge separation. LNO can reduce separation and promote cell stability.	[97]
LCO|LiPON	XPS	The experiment-supported energy level diagram indicates the presence of a space charge layer	[93]
/	Mathematical model+constitutive assumption	The predicted SCL is one order of magnitude larger than that in LE, and is mainly determined by dielectric properties of SE	[36]
$Li_xV_2O_5$|LAGP	2D-EXSY NMR	The SCL leads to a significant increase in the activation energy for Li-ion diffusion over the interface	[23]
LCO|LLZO/LATP|graphite	Theoretical model (Coulombic interactions)	The SCL with a thickness in nanometer regime, causing a small resistance, thus having a negligible effect	[90]
LCO(104)|LPS(010)	CALYPSO+DFT	Interfacial Li^+ sites with higher $\mu_{Li}(r)$ values cause dynamic Li^+ depletion, which can allow oxidative decomposition of SE materials.	[98]
NCM|ipn-PEA (LATP)	AFM interfacial potential measurements	The coating layer provides a gradual potential slope, mitigates polarization and weakens SCL	[95]
LCO|β-Li_3PS_4 (LNO)	DFT+U calculations	The LNO buffer layer suppresses the growth of SCL by eliminating interfacial Li adsorption sites	[35]
$LiCoO_2$|Li_6PS_5Cl ($BaTiO_3$)	Differential phase contrast scanning transmission electron microscopy (DPC-STEM)	Interface lithium-ion accumulation resulting from the SCL, $BaTiO_3$ coating could reduce this effect.	[99]

indicated the role of SCL was dynamically changing during cycling. In a very recent work, Cheng *et al*. [23] used two-dimensional exchange spectroscopy (2D-EXSY) nuclear magnetic resonance (NMR) to check the $Li_xV_2O_5$|LAGP interface during cycling. It demonstrated that the space-charge effect significantly increased the Li ion diffusion activation energy by more than 2 times, which offered a quantitative measurement on the effect of SCL, as is shown in Figure 4(d).

2.4.3 Solutions to SCL

Although how the SCL affects interface charge transfer process is unclear, it is reported that the protective coatings are effective to eliminate the space charge phenomena at ED|SE interfaces. Ohta *et al*. [96] thought that the large difference of chemical potentials would drive the Li^+ ions to transfer from the solid electrolyte to $LiCoO_2$, thus developing a space-charge layer with high resistance at interfaces, and a slope prior to the theoretical plateau arose on the charging curve. Bringing in an artificial thin film, such as $Li_4Ti_5O_{12}$, would shield the slope, suggesting that this coating could suppress the beginning space charge transfer process and the resultant formation of SCL. Haruyama *et al*. [35] investigated the LCO|LPS, LCO|LNO and LNO|LPS interfaces by using the DFT+U methods. The calculated results indicated that Li atoms tended to adsorb on the LCO surface, which led to the formation of the equilibrium SCL and high interfacial resistance, while the LNO interposition eliminated Li adsorption sites and suppressed the growth of Li depletion zone. Liang *et al.* [95] measured the boundary potential distribution of the coated $LiNi_{0.6}Co_{0.2}Mn_{0.2}O_2$ (NCM 622) by AFM, and revealed that the formed interfacial transition layer provided a gradual potential slope and sustain-released polarization and endowed the battery with improved cycling stability (Figure 4(e)). Recent experimental researches on space charge issues are summarized in Table 2, which demonstrates that the coatings can effectively suppress the development of SCL, but the reasons behind this still need to be clarified. Especially, how coatings affect the distribution of charge carriers.

2.5 Contact and mechanical stability

The working of batteries relies on the transportation of ions within the battery and electrons in external circuit. Hence, an effective percolation network between active materials, conductive additives, electrolytes (liquid or solid), and current collectors needs to be well bridged. In traditional lithium-ion batteries, the flowing liquid electrolyte can spontaneously wet the surface of active materials and enable a fast ion flux across the electrode|electrolyte interface. Thus, in most of scenario, the charge transfer process across the interface could not be a serious limiting step. In solid-state batteries, the immobile and stiff nature of solid electrolytes makes it hard to enable compact contact interfaces [100]. Insufficient contact will result in low concentration of effective electrochemical active sites, making the ion flux bundle together to transport across the electrode|electrolyte interface, which has been interpreted as a strong indication of transport kinetic limitation in batteries. Worse still, even if a

perfect interface is built in the beginning, the contact can change dynamically as the volume changes of electrode materials and growth of interphases during cycling will also play an important mechanical role.

2.5.1 Physical contact

Solid electrolytes, because of their rigid nature and illiquidity, can hardly compromise with electrode surface or active particles spontaneously, so the realistic interfaces are often a mixture of porosity and micro-contacts considering the weak interactions between SE and active particles. In fact, the true contact area is far less than the apparent, geometrical connection surface, which reduces the number of electrochemical active sites at the interface. As a consequence, lithium ion flux is restricted in limited local spots, called current constriction [55]. It is clearly that the insufficient contact will dominate the measured huge interface resistance according to equation (4). The huge contact resistance will not only increase the ohmic polarization and restrict the rate performance, but also lead to high local current density at these limited contact points and finally lead to the growth of lithium dendrites. This is even more serious by using solid oxide electrolytes whose Young's modulus is typically higher than sulfide electrolytes.

(1) Lithium metal anode side

Lithium metal has been grabbing attention because of its low potential and high capacity. The severe side reactions, huge volume effect during plating and stripping, and dendrite issues hindered its applications in traditional liquid-electrolyte based batteries [101,102]. People pin their hopes on solid-state lithium batteries because of the high shear modulus of solid electrolytes, which is thought to obstruct the penetration of lithium dendrites. However, it is found that solid electrolytes are more prone to forming dendrites than liquid electrolytes [103]. The reasons for the dendrite growth are various, including low relative density, pre-existing defects, high interfacial resistance, which have been systematically discussed in a recent review [10]. Here we will only discuss the insufficient interfacial contact induced inhomogeneous plating.

The Li|SEs interfacial contact resistance comes from two aspects. One is induced by the poor bonding attraction. Garnet-type oxide electrolytes show extremely poor wettability with lithium metal. Recent studies indicate that the surface contaminant, Li_2CO_3, is the crime culprit for this and many corresponding methods have been put forward, including fast acid treatment or tempering to remove this contaminant layer [104,105]. High pressure can also improve the connection and lower contact resistance. For example, the total impedance of a Li|Li_6PS_5Cl|Li symmetric cell can exceed 500 Ω under a low loading pressure of 1 MPa. This value decreases to ~110 Ω at 5 MPa, ~50 Ω at 10 MPa, 35 Ω at 20 MPa, and 32 Ω at 25 MPa. When the pressure is recovered to 5 MPa, the impedance only increases to ~50 Ω [106] as shown in Figure 5(a–c), which is only half of the initial value under the same pressure, suggesting the importance of pressure on improving contact during the assembling process.

Another aspect of contact resistance arises from the morphological instability during the cycling. A fundamental problem is void formation at the interface by using metal electrodes in SSLBs. Kirkendall voids are speculated to be formed during the striping process because of the sluggish mass transfer of lithium metal and insufficient applied-pressure to replenish the dissolved lithium. These voids will definitely affect the interfacial resistance but it is hard to isolate the dissolution-related resistance with a two-electrode configuration [27]. Sakamoto's group [27] and Bruce's group [103] investigated the dynamic polarization of the plating and stripping processes and their correlation with applied stack pressure and current density by using a three-electrode configuration cell. It was found that the overpotential of a symmetric cell during cycling mainly came from the dissolution process. Under anodic operating condition if the stripping current density exceeds the rate of replenishing lithium, vacancies will form and accumulate at the interface and eventually merge into void spaces, resulting in the loss of contact area. As a consequence, the local current at the remaining contact points can be very high, which further accelerates the growth of voids. Therefore, it is necessary to counteract the problem of void formation in order to avoid contact loss. Several ideas have been proposed to maintain sufficient connection between lithium metal and electrolytes. Sakamoto *et al.* [27] put forward the concept of "critical stack pressure". The critical stack pressure is defined as the pressure at which the flux of incoming lithium induced by the applied stack pressure is equal to the flux of lithium dissolved into electrolytes. If the applied pressure is higher than the critical stack pressure, the interfacial contact and morphological stability can be kept, as shown in Figure 5 (g). Otherwise, voids will be formed at the lithium|electrolyte interface, as shown in Figure 5(h). For example, the critical stack pressure of a Li|LLZO|Li symmetric cell for the stable cycling at 0.1, 0.2, and 0.4 mA cm^{-2} is 0.4, 1.2, and 2.0 MPa, respectively. The three-electrode experiment provides strong evidence about this, as shown in Figure 5(i). The potential of working electrodes and counter electrodes can be deconvoluted by using a Ni reference electrode. A noticeable increase of potential can be observed on the working electrode (lithium stripping process), while the counter electrode (lithium plating process) remains flat. These results strongly indicate that the observed polarization is mainly due to the formation of voids during the stripping process [27]. It should be pointed out that this does not mean that the higher pressure the better. Although the interfacial resistance decreases to nearly 0 Ω cm^2 at higher external pressure for a Li|LLZO|Li

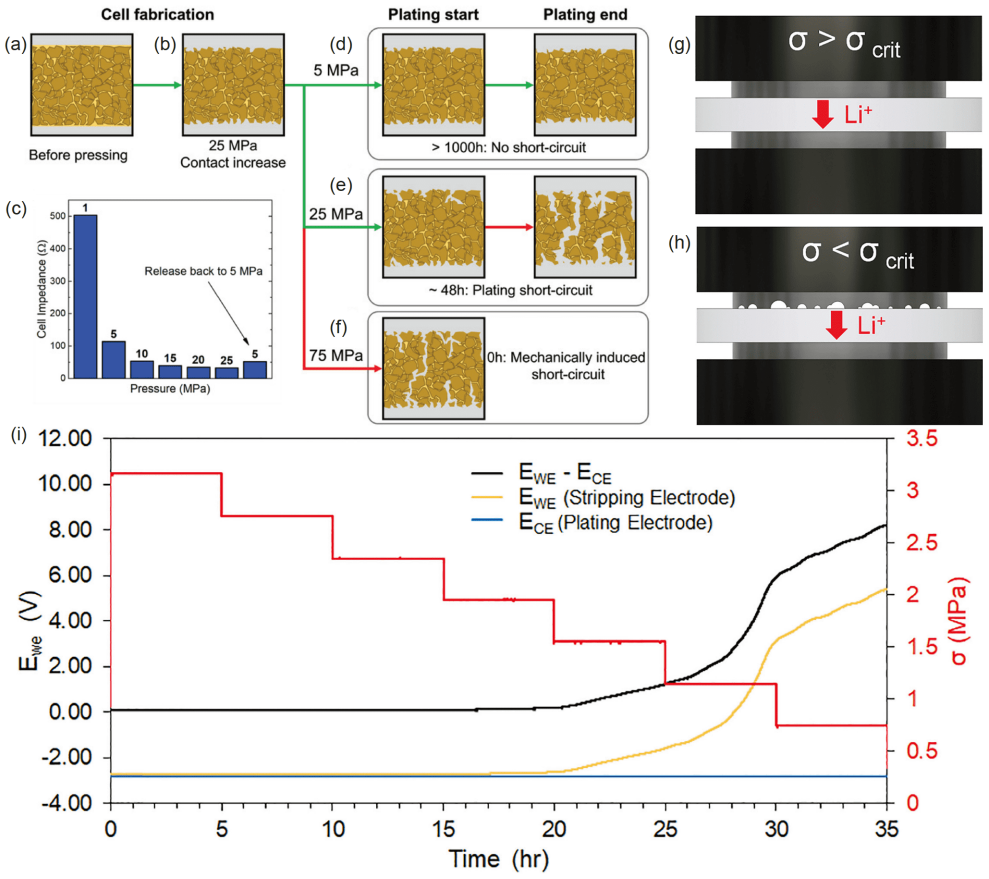

Figure 5 (a–f) Stack pressure on the shorting behavior of lithium-metal SSBs: (a) poor contact of electrolytes and lithium before pressing; (b) 25 MPa is applied to press the lithium metal on electrolytes; (c) the cell resistance decreased a lot even after the pressure is recovered to 5 MPa; (d) 5 MPa, (e) 25 MPa, (f) 75 MPa is applied on the symmetric cell during the cycle [106]. (g–h) Depletion of Li at the Li|electrolyte interface during cycling: (g) above the "critical stack pressure", the applied pressure is sufficient to maintain the contact between lithium and electrolytes; (h) below the "critical stack pressure", the applied pressure is insufficient to replenish lithium at the interface, leading to void formation at the interface and reduction of contact area; (i) potential response under a constant current density of 0.2 mA cm^{-2} and decreasing stack pressure [27] (color online).

symmetric cell [49], for a Li|Li_6PS_5Cl|Li system, too high stack pressure will lead to the lithium creeping along the grain boundary and fast shortening of the lifetime of the cell after several cycles (25 MPa), or directly mechanical shorting (75 MPa) as shown in Figure 5(e, f). This difference may arise from the different mechanical properties of electrolytes. The relative density of garnet ceramic pellet made by high-temperature sintering is usually higher than 95% while the sulfide electrolyte pellet made by cold-press still possesses 18% porosity even at high pressure [106]. Thus, the choice of applied pressure must consider the different properties of electrolytes and make a trade-off with engineering as high-pressure equipment will also lower the energy density of pack. Another effective method is increasing diffusion kinetics of lithium metal. Thorben *et al*. [107] found that introducing 10% Mg into lithium metal could effectively prevent contact loss because of the higher effective diffusion coefficient (Figure 6). Nevertheless, there still exists a fundamental kinetic limitation in the Li-rich alloy due to the decreased lithium concentration at the interface. When the stripping current density exceeds 1 mA cm^{-2}, a higher temperature is required to enable the high lithium utilization.

(2) Cathode side

The physical contact between solid electrolytes and cathodes is generally worse than that on the anode side. The excellent plastic deformation ability of lithium metal makes it possible to achieve good contact with an electrolyte layer by a high pressure or melting method. However, mainstream cathodes, such as transition metal layered oxides, possess high Young's modulus and could not topologically compatible with the stiff solid electrolyte. It is now still a remaining challenge to obtain an enough cathodic-active path in oxide-based SSLBs.

Several interface engineering methods have been proposed to bridge a continuous conduction path in composite cathodes and at cathode|oxide electrolyte interfaces. For example, ionic liquid can act as mass transfer media and is added to the cathode side by virtue of its nonflammability, nonvolatility and high viscosity [108]. Sintering method can densify the composite electrode and help form proper ceramic bonding at the electrode|electrolyte interface. However, the required high fusing temperature brings serious chemical

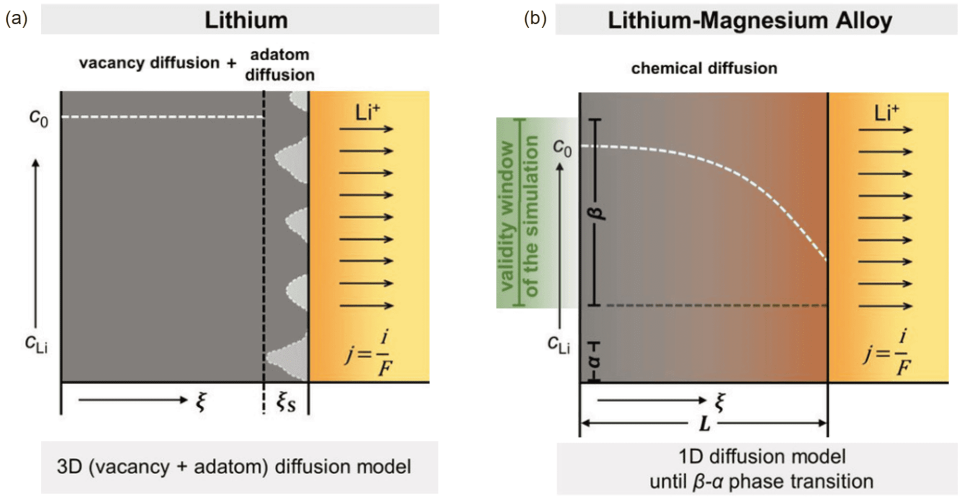

Figure 6 Lithium transport properties and morphological change of the interface between solid electrolytes and (a) lithium metal electrodes and (b) a lithium rich Li-Mg alloy electrodes [107] (color online).

diffusion and leads to the formation of high resistance layers, even with an advanced sintering method [109]. Figure 7(a) demonstrates the elemental cross-diffusion across the $LiCoO_2$|LLZO interface induced by high-temperature processing [75]. Sintering aid agents which act as an interfacial binder can help form a close cathode|electrolyte interface at a relative low temperature. For example, the introduction of Li_3BO_3, with a low melting point ~700 °C, into LLZO and $LiCoO_2$ interfaces can improve the physical bonding and reduce chemical cross-contamination [75, 106,110,111]. Further, Han *et al*. [31] ingeniously utilized the reaction between $Li_{2.3}C_{0.7}B_{0.3}O_3$ (LCBO) and the naturally formed Li_2CO_3 to solder $LiCoO_2$ and LLZO together, as shown in Figure 7(b). The obtained all-solid-state Li|LLZO|LCO batteries exhibit high rate performances and decent cycle performances (100 cycles at 25 °C). Polymer interlayers are also adopted to improve the poor solid-solid contact [108,112]. Liang *et al*. [113] engineered Janus interfaces on ceramic electrolytes, as shown in Figure 7(d). Polyacrylonitrile (PAN) with high voltage stability and polyethylene oxide (PEO) with high stability against lithium metal are used to bind the cathode and anode with LATP ceramic, respectively. Three-dimensional interface structure design is also beneficial for the intimate contact of electrolytes and electrode materials by increasing the contact area [114,115]. Some liquid and organic electrodes have their natural advantages in addressing the interfacial contact problem and will be important topics in the future [116–118].

By contrast, the physical contact between cathode and sulfide electrolytes is generally better than that with oxide electrolytes because of the much softer feature. High-quality percolation pathway can be obtained by pressing composite electrodes onto a sulfur electrolyte layer. Interestingly, the cathode particle size was found to affect the electronic contact and therefore the utilization ratio of active materials. Composites made from small particles can provide more contact points than those from large particles [119]. However, the change of cell volume of electrolyte materials during the delithiation will lead to irreversible contact loss [120]. The mechanical failure during cycling will be discussed in detail in the following part.

2.5.2 *Mechanical compatibility during the cycling*

Mechanical breakdown has been widely discussed in traditional batteries with liquid electrolytes. The related crack in the cathode, anode and solid electrolyte interphase is regarded as one of the main failure mechanisms [121]. In a liquid system, the plastic binder and fluid electrolytes can disperse and accommodate the mechanical stress and alleviate the mechanical damage to some extent [24]. However, because of the incompressibility of SEs, the generated stress will be directly exerted on contact sites and lead to cracking or delamination of the junction, and the active materials become partially inactive in this situation, thus contributing to the overall capacity loss. Besides, the aforementioned fracture within the active materials, the huge internal stress also tends to fracture the electrolyte pellet. It is highlighted that the electro-chemo-mechanical stability become more prominent and can change the capacity and diffusivity of the cells through the induced internal stress. Understanding and controlling the origin of stress, the strain on ion-transport pathways and volumetric deformation, and the tolerance of related materials can be a key to improve the performance of batteries.

(1) Origin of the mechanical mismatch and its effects

The origin of the mechanical stress can be basically divided into two categories: expansion and contraction of the electrode materials; volumetric change caused by the formation of interphase. The former comes from the intrinsic crystallographic contraction/expansion of electrode materi-

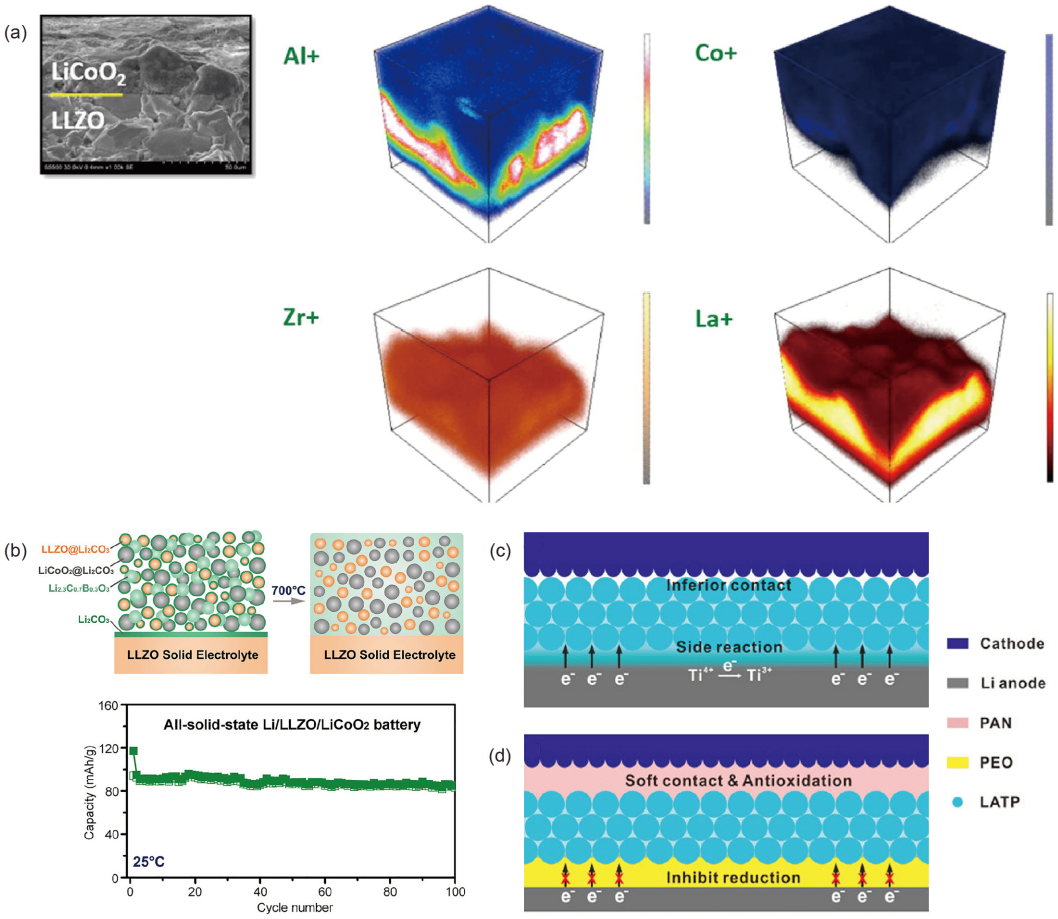

Figure 7 (a) Three-dimensional elemental mapping of the $LiCoO_2$|LLZO interface obtained by time of flight secondary ion mass spectrometry (TOF-SIMS), color scales beside the maps show ionic concentrations of each ions: upper represents a higher concentration [75]. (b) Schematic of the LCBO interphase engineered all ceramic LCO|LLZO interfaces and the cycle performance of the interphase-engineered all-ceramic Li|LLZO|LCO battery at 0.05 C at 25 °C [31]. Illustration of the solid-state full battery with (c) pristine LATP electrolytes and (d) disparate-polymer-engineered LATP electrolytes [113] (color online).

als during lithiation/de-lithiation. The later arises from the side reaction between electrodes and electrolytes and its evolution is strongly related with electrochemical transport properties.

Most electrode materials suffer severe volume changes during charging/discharging. For example, NCM 811 undergoes up to 7% contraction when it is charged to 4.3 V. As for graphite, the volume strain can reach 13% with full lithiation to LiC_6. The continuous swelling and contraction of electrodes can lead to the delamination and crack of particles. In liquid electrolytes, such cracks can be filled by fluidic electrolytes and boost faster charge transfer kinetics by increasing the electrochemically active surface. However, these cracks are detrimental for solid state batteries by degrading the corresponding kinetics [122]. Giovanna *et al.* [123] quantitatively assessed the mechanical reliability in solid state batteries for the first time. For a solid electrolyte with Young's modulus E_{SE}=15 GPa and bulk fracture energy G_c=1.0 J m^{-2}, which are representative values for sulfides, the simulation indicates that cracks initiate when particles undergo only 3% volume change, suggesting the high likelihood of mechanical failure in solid state batteries. Contact loss has been observed experimentally in a sulfide electrolyte solid battery (Figure 8(a–d)). The mechanical contraction of active cathode materials during charging contributed to contact loss between active material particles and electrolytes, which increases internal resistance and expedites capacity fading of batteries [26,120]. These problems can be aggravated at some extremely harsh conditions, like overcharging. The mechanical stress will also pose a serious threat to electrolyte itself. For instance, in a solid-state battery with LCO and indium as a cathode and an anode, respectively, bending and cracking of the solid electrolyte pellet is observed because of the generated macroscopic strain during cycling [124].

As we have discussed in section 2.2, the formation of interphase is unavoidable in most SSLBs, and the growth of interphase can also induce mechanical stress in the system. Tian *et al.* [28] evaluated the mechanical stress in SSLB with a finite-element method. With two sources of mechanical

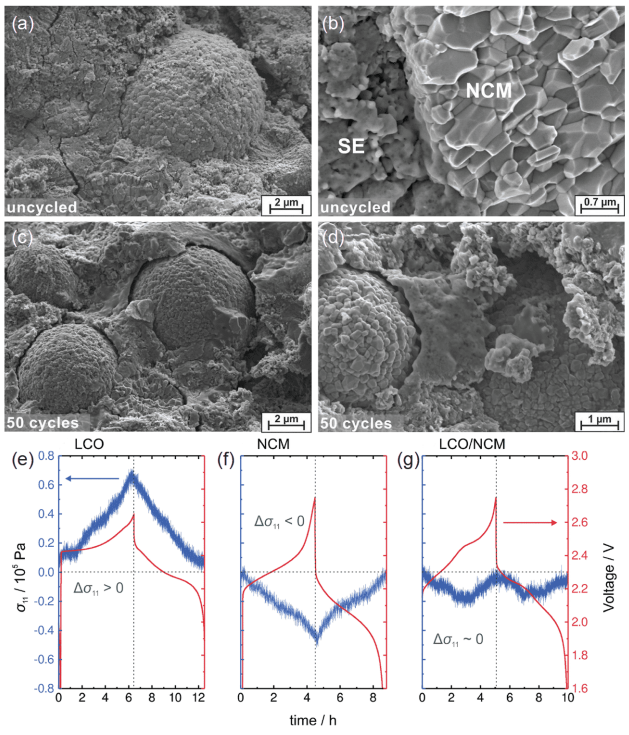

Figure 8 (a–d) Scanning electron microscopy (SEM) images of the cathode composite of NCM 811 and β-Li_3PO_4: (a, b) as prepared without applied current or potential; (c, d) SEM inages of the cell after 50 cycles in the discharged state [120]. Comparison of the stress response of LTO/SE|SE|CAM/SE using (e) LCO, (f) NCM-811 and (g) a blend of 55:45 wt.% NCM-811:LCO cathode composites. The cell with LCO shows positive volume expansion effects. The cell with NCM-811 exhibits a negative stress response. However, the cell containing the blending of LCO and NCM-811 shows an overall lower nominal stress [24] (color online).

variation, expansion/contraction of electrode materials and interphase-formation-related volumetric change were considered. It is found that the decomposition-reaction-contributed stress can be more remarkable. The stress induced by the expansion of silicon electrodes and LCO electrodes during charging only affects the surface layer of LCO and that inside LiPON near silicon. On the other hand, if the interfacial reaction is not self-limiting and the thickness of interphases keeps growing (*i.e.*, MIC-type), the volume expansion of such interphases can produce a huge stress inside the electrolyte and finally break up the electrolyte pellet, as has been observed at LATP|Li interfaces in our recent work [20].

(2) Solutions to the mechanical instability

The discussed mechanical limitations can be circumvented by material or structural design and interface engineering. Considering the origin of mechanical instability, one effective approach is to develop zero-strain (or quasi zero-strain) electrode materials. For example, $Li_4Ti_5O_{12}$ was used as an anode in SSLB and exhibited a smaller mechanical stress [24]. Future research could be further devoted to developing new zero-strain electrode materials, such as $LiNi_{0.2}Co_{0.7}Mn_{0.1}O_2$, $LiCaFeF_6$, spinel $LiCoMnO_4$ and $Li_2Ni_{0.2}Co_{1.8}O_4$ [125–128]. Also, we can utilize the different cell volume variation characteristics of electrode materials to balance the mechanical mismatch by exploring binary or ternary composite cathode materials. For instance, the cell volume of LCO undergoes expansion upon charging while nickel-rich cathodes suffer shrinkage. By combining LCO and NCM 811 as a composite cathode, the generated stress can be much alleviated, as shown in Figure 8(e–g) [24]. In addition, although the delamination is thought to be independent of the particle size, the delamination of nanoparticles can proceed smoothly and the crack growth may not reach completion [123]. Additionally, the introduction of flexible components to the electrodes or electrolytes can also buffer the generated stress.

3 Advanced characterization techniques for electrode|electrolyte interfaces in SSLBs

Various characterization techniques and their combinations have been applied to uncover the relationship between the ED|SE interfacial degradation and the performance of the solid-state batteries. However, two main obstacles hinder the interfacial characterization process in SSLBs: sample preparation and availability of characterization techniques. The former lies in the fact that these interfaces are usually buried inside the battery. Unlike the liquid electrolyte-based batteries, in which the electrolyte can be easily washed away, the interface related information in solid state batteries is usually covered by electrolyte and hard to be extracted. In addition, due to the sensitivity of electrolyte or electrode materials to air and moisture, the preparation process needs to be operated under the protection of inert atmosphere. The latter consideration lies in the fact that conventional characterization techniques only provide average information over a large spatial range. However, the realistic interfacial region is within several hundreds of nanometers, with complex nanostructures and chemistry distribution. More powerful techniques and appropriate designs are desired to extract and amplify the interfacial signals.

Successful sample preparation is the first key step to fully reflect what is truly taking place at the ED|SE interface. *Ex-situ* characterization techniques usually require a post-processing to preserve the essential features of the interface structure. However, this process is not easy to be implemented, especially for sensitive samples like Li metal and sulfide electrolytes. Thus, an advanced sample preparation method is expected. To avoid possible damage from sample making process and high-energy electron/ion beam, Meng *et al.* [11] used cryo-electron microscopy (Cryo-EM) to probe the potential stabilization mechanism of Li|LiPON interfaces. A Li|LiPON sample was prepared by Cryo-focused ion beam (Cryo-FIB), and then the TEM samples were made

based on "Cryo-lift-out" technology. Analysis results show that a unique multilayer mosaic-like SEI structure is formed at this interface.

Advances in technologies have brought a variety of choices and richer results to our experiments. Some traditional techniques like infrared spectroscopy and Raman spectroscopy are unsuitable to directly obtain correlated signals. Although X-ray can penetrate solid electrolytes, the local interphase is usually composed of amorphous phase and the weak signals may be overwhelmed within the bulk signal. Thus, traditional X-ray diffraction (XRD) can only provide limited information about the interphase. By contrast, microscopic techniques can be used to monitor local structural and chemistry changes. Liu *et al.* [129] employed X-ray full-field transition microscopy imaging combined with X-ray absorption near-edge structures (FF-TXM-XANES) to reveal the 3D evolution of the cracks and their successive impact on local-ion transport within $LiNi_{0.8}Co_{0.15}Al_{0.05}O_2$ (NCA) electrode particles, which provided valuable information about the battery degradation mechanism under realistic operation conditions. Lewis *et al*. [130] revealed the evolution of lithium|solid electrolyte interfaces during cycling with *operando* synchrotron X-ray computed microtomography. Direct visualization of interphase growth and loss of contact provide us more insight on chemo-mechanics and its effects in solid-state batteries. Otherwise, new emerging applications can also provide richer information of the interfaces in SSLBs. Solid-state nuclear magnetic resonance (SS-NMR) can directly detect the signal of nucleus regardless of the existing form of interphase, either crystalline, amorphous, or covered with electrolytes. In addition to directly detecting the composition and chemical information of interphases, the lithium-ion diffusion kinetics and dynamic evolution of interfaces in SSLBs can be quantitatively characterized by the derived related techniques. For example, Zhou *et al.* [23] revealed the effect of the space charge layers on the ion migration over the interface with two-dimensional exchange (2D-EXEY) NMR by controlling the lithium chemical potential difference between $Li_xV_2O_5$ electrodes and $Li_{1.5}Al_{0.5}Ge_{1.5}(PO_3)_4$ (LAGP) electrolytes. Table 3 lists the present characterization techniques that can investigate interface behaviors and provides a brief description of the obtained information of each technique. More details on specific techniques or more general applications in interface researches can be found in the recent literature [131–134].

4 Summary and future perspectives

To summarize, extensive studies have already highlighted the importance of several factors when the compatibility and the kinetics of the electrode|soild electrolyte interface in SSLBs are considered. However, it is often too complicated to clearly assign individual process and its effect on battery's performances. From this point of view, we detach the crucial interfacial limitation that seriously affects the performances of SSLBs. Fundamental concepts and their effects on charge transfer process are parsed based on thermodynamics, kinetics and mechanics, which can help further understand the evolution of interfaces and relationships of interface-resistance.

Even though people have gained a better understanding of the transport processes at ED|SE interfaces with the help of advanced experimental and computational methods in the last decades, the truth of the interfacial behaviors still remains an open question. Especially, the matching issues of electrochemical stability windows, charge transfer mechanisms across the interface and mechanical mismatch solutions between electrode materials and rigid solid electrolytes are waiting for update. Nevertheless, a further comprehension of the complex interfacial behaviors is urgently desired. Future

Table 3 Summary of the characterization techniques on interface researches

	Techniques	Main information
Photon	Optical microscope	Morphology
	Raman	Surface structure, constituent
Electron	SEM/(S)TEM/EDS/EELS	Morphology, element distribution, valence state
	Electron hologram (EH)	Potential distribution
X-ray	XRD	Chemical constituents, structures
	XPS	Surface chemical information
	XAS	Chemical information
	X-ray tomography	Microstructures
Neutron	Neutron depth profile (NDP)	Element distribution
Radio frequency	SS-NMR	Chemical information, diffusion dynamics
Mass spectrum	TOF-SIMS	Constituent/Element distribution
Calculation	DFT (+simulation)	Structure, constituent, chemical information

breakthroughs need to be taken into account of the following points:

(1) *Detaching and quantifying different process*. To provide convincible proofs, the experimental design should isolate individual factors or provide enough comparative analysis. For example, from a thermodynamic point of view, the differences of chemical potentials between electrode materials and solid electrolytes will inevitably lead to interphase formation or element mutual diffusion and rearrangement of interfacial carriers. Hence, it is hard to discriminate the effect of SCLs with interphases or diffusion layers. On the other hand, microscopic features analysis, quantitative and dynamic estimation are urgently needed in order to elaborate the effect of these phenomena.

(2) *Developing suitable theoretical models*. Although great achievements have been made in computational estimation and modeling, the simplified models can rarely unify the simulated results with experimental phenomena in most situations. For example, kinetic considerations also determine whether, how fast, and which interfacial products are formed, but the interfacial kinetic calculation is still unavailable at the present stage. Also, modeling on space charge phenomena is based on the typical electric double layer theory under the diluted solution approximation. It is now unclear whether the derived equations can directly apply to the solid|solid interfaces or not. In addition, mechanical evolution of interfaces during electrochemical cycling is also a key factor that controls the performance of SSLBs. However, the corresponding modeling is still vacant. To provide in-depth insights into the underlying failure mechanisms at ED|SE interfaces, the developing model should also take the kinetics, mechanics and microstructural features into consideration.

(3) *More advanced characterization techniques*. As we can see that current characterization techniques can hardly access to the buried interface, and fewer can provide microstructure information. Future developing techniques could provide more nucleation, structural and compositional information at atomic scale. *In-situ* and/or *operando* experiments with high spatial-temporal resolution are highly expected to dynamically reveal the chemical and structural evolution. Besides, nondestructive and quantifiable techniques, like SS-NMR, will provide significant help to uncover essential scientific problems at ED|SE interfaces.

(4) *Designing a stable interface*. Interfacial engineering strategies of applying artificial coating layers were accepted to effectively improve the interfacial stability and electrochemical performances of SSLBs. But the specific roles and the required properties of these coatings are unclear, and need more estimation to offer guidance for future strategy design. On the other hand, the mechanical stress issues also pose a serious threat to the cycling performance but the answer is still up in the air. Hence, there is a need to design a proper interfacial modification strategy to improve the thermodynamical and kinetical stability, as well as the morphological stability.

(5) *Grasping key factors*. What are the main limitations at the interface varying from scene to scene in different types of SSLBs? For examples, for oxide electrolytes, we mainly focus on the physical contact with electrodes in present stage. The bond between electrolytes and electrode materials is too weak to provide enough percolation networks for successful working. For sulfides, stability issues and SCL problems dominate the agenda, and which one is responsible for the fast degradation is still in debate. And the effect of mechanical stress cannot be ignored in both systems. Hence, the origin of high interfacial resistance and sluggish charge transfer needs to be carefully checked at different interfaces.

All in all, many scientific and technological challenges still remain at present. Enhancement of compatibility and reduction of interfacial resistivity are the critical steps to achieve advanced SSLBs, which relies on a full understanding of the essential scientific problems. Innovative experimental methods, powerful computational methods and advanced characterization techniques will provide critical new insights to these complex interfacial phenomena and shed light on the design and optimization of future solid-state lithium batteries.

Acknowledgements This work is financially supported by the National Key Research and Development Program of China (grant no. 2018YFB0905400), the National Natural Science Foundation of China (21935009).

Conflict of interest The authors declare no conflict of interest.

1 Tarascon JM, Armand M. *Nature*, 2001, 414: 359–367
2 Goodenough JB, Park KS. *J Am Chem Soc*, 2013, 135: 1167–1176
3 Janek J, Zeier WG. *Nat Energy*, 2016, 1: 16141
4 Manthiram A, Yu X, Wang S. *Nat Rev Mater*, 2017, 2: 16103
5 Zhang Z, Shao Y, Lotsch B, Hu YS, Li H, Janek J, Nazar LF, Nan CW, Maier J, Armand M, Chen L. *Energy Environ Sci*, 2018, 11: 1945–1976
6 Kato Y, Hori S, Saito T, Suzuki K, Hirayama M, Mitsui A, Yonemura M, Iba H, Kanno R. *Nat Energy*, 2016, 1: 16030
7 Yang X, Adair KR, Gao X, Sun X. *Energy Environ Sci*, 2021, 14: 643–671
8 Luntz AC, Voss J, Reuter K. *J Phys Chem Lett*, 2015, 6: 4599–4604
9 Takada K, Ohta N, Tateyama Y. *J Inorg Organomet Polym*, 2015, 25: 205–213
10 Cao D, Sun X, Li Q, Natan A, Xiang P, Zhu H. *Matter*, 2020, 3: 57–94
11 Cheng D, Wynn TA, Wang X, Wang S, Zhang M, Shimizu R, Bai S, Nguyen H, Fang C, Kim M, Li W, Lu B, Kim SJ, Meng YS. *Joule*, 2020, 4: 2484–2500
12 Usiskin R, Maier J. *Adv Energy Mater*, 2021, 11: 2001455
13 Wang D, Zhu C, Fu Y, Sun X, Yang Y. *Adv Energy Mater*, 2020, 10: 2001318
14 Chen R, Li Q, Yu X, Chen L, Li H. *Chem Rev*, 2020, 120: 6820–6877
15 Yang X, Luo J, Sun X. *Chem Soc Rev*, 2020, 49: 2140–2195
16 Banerjee A, Wang X, Fang C, Wu EA, Meng YS. *Chem Rev*, 2020, 120: 6878–6933

17 Schwietert TK, Arszelewska VA, Wang C, Yu C, Vasileiadis A, de Klerk NJJ, Hageman J, Hupfer T, Kerkamm I, Xu Y, van der Maas E, Kelder EM, Ganapathy S, Wagemaker M. *Nat Mater*, 2020, 19: 428–435
18 Zhao Q, Stalin S, Zhao CZ, Archer LA. *Nat Rev Mater*, 2020, 5: 229–252
19 Zheng B, Liu X, Zhu J, Zhao J, Zhong G, Xiang Y, Wang H, Zhao W, Umeshbabu E, Wu QH, Huang J, Yang Y. *Nano Energy*, 2020, 67: 104252
20 Zhu J, Zhao J, Xiang Y, Lin M, Wang H, Zheng B, He H, Wu Q, Huang JY, Yang Y. *Chem Mater*, 2020, 32: 4998–5008
21 Tateyama Y, Gao B, Jalem R, Haruyama J. *Curr Opin Electrochem*, 2019, 17: 149–157
22 Swift MW, Qi Y. *Phys Rev Lett*, 2019, 122: 167701
23 Cheng Z, Liu M, Ganapathy S, Li C, Li Z, Zhang X, He P, Zhou H, Wagemaker M. *Joule*, 2020, 4: 1311–1323
24 Koerver R, Zhang W, de Biasi L, Schweidler S, Kondrakov AO, Kolling S, Brezesinski T, Hartmann P, Zeier WG, Janek J. *Energy Environ Sci*, 2018, 11: 2142–2158
25 Pervez SA, Cambaz MA, Thangadurai V, Fichtner M. *ACS Appl Mater Interfaces*, 2019, 11: 22029–22050
26 Sun N, Liu Q, Cao Y, Lou S, Ge M, Xiao X, Lee WK, Gao Y, Yin G, Wang J, Sun X. *Angew Chem Int Ed*, 2019, 58: 18647–18653
27 Wang MJ, Choudhury R, Sakamoto J. *Joule*, 2019, 3: 2165–2178
28 Tian HK, Chakraborty A, Talin AA, Eisenlohr P, Qi Y. *J Electrochem Soc*, 2020, 167: 090541
29 Han F, Zhu Y, He X, Mo Y, Wang C. *Adv Energy Mater*, 2016, 6: 1501590
30 Urban A, Seo DH, Ceder G. *npj Comput Mater*, 2016, 2: 16002
31 Han F, Yue J, Chen C, Zhao N, Fan X, Ma Z, Gao T, Wang F, Guo X, Wang C. *Joule*, 2018, 2: 497–508
32 Maier J. *Berichte der Bunsengesellschaft für physikalische Chem*, 1985, 89: 355–362
33 Schmalzried H, Janek J. *Berichte der Bunsengesellschaft für physikalische Chem*, 1998, 102: 127–143
34 Santhanagopalan D, Qian D, McGilvray T, Wang Z, Wang F, Camino F, Graetz J, Dudney N, Meng YS. *J Phys Chem Lett*, 2014, 5: 298–303
35 Haruyama J, Sodeyama K, Han L, Takada K, Tateyama Y. *Chem Mater*, 2014, 26: 4248–4255
36 Braun S, Yada C, Latz A. *J Phys Chem C*, 2015, 119: 22281–22288
37 Lewis JA, Tippens J, Cortes FJQ, McDowell MT. *Trends Chem*, 2019, 1: 845–857
38 Zhao Y, Stein P, Bai Y, Al-Siraj M, Yang Y, Xu BX. *J Power Sources*, 2019, 413: 259–283
39 Yang Y. *Solid State Electrochemistry*. Beijing: Chemical Industry Press, 2016. 1–6
40 Brad A, Faulkner L. *Electrochemical Methods: Fundamentals and Applications*. New York: John Wiley & Sons, Inc., 2000
41 Weiss M, Simon FJ, Busche MR, Nakamura T, Schröder D, Richter FH, Janek J. *Electrochem Energ Rev*, 2020, 3: 221–238
42 Han F, Westover AS, Yue J, Fan X, Wang F, Chi M, Leonard DN, Dudney NJ, Wang H, Wang C. *Nat Energy*, 2019, 4: 187–196
43 Li F, Li J, Zhu F, Liu T, Xu B, Kim TH, Kramer MJ, Ma C, Zhou L, Nan CW. *Matter*, 2019, 1: 1001–1016
44 Dudney NJ, West WC, Nanda J. *Handbook of Solid State Batteries*. World Scientific, 2015
45 Iriyama Y, Kako T, Yada C, Abe T, Ogumi Z. *Solid State Ion*, 2005, 176: 2371–2376
46 Kobayashi Y. *Solid State Ion*, 2002, 152-153: 137–142
47 Ohta S, Kobayashi T, Seki J, Asaoka T. *J Power Sources*, 2012, 202: 332–335
48 Buschmann H, Berendts S, Mogwitz B, Janek J. *J Power Sources*, 2012, 206: 236–244
49 Krauskopf T, Hartmann H, Zeier WG, Janek J. *ACS Appl Mater Interfaces*, 2019, 11: 14463–14477
50 Yu C, Ganapathy S, Eck ERH, Wang H, Basak S, Li Z, Wagemaker M. *Nat Commun*, 2017, 8: 1086
51 Eyring H, Lin SH. *Basic Chemical Kinetics*. John Wiley & Sons, Inc., 1980
52 Richards WD, Miara LJ, Wang Y, Kim JC, Ceder G. *Chem Mater*, 2015, 28: 266–273
53 Otoyama M, Ito Y, Hayashi A, Tatsumisago M. *J Power Sources*, 2016, 302: 419–425
54 Auvergniot J, Cassel A, Ledeuil JB, Viallet V, Seznec V, Dedryvère R. *Chem Mater*, 2017, 29: 3883–3890
55 Krauskopf T, Richter FH, Zeier WG, Janek J. *Chem Rev*, 2020, 120: 7745–7794
56 Fu KK, Gong Y, Fu Z, Xie H, Yao Y, Liu B, Carter M, Wachsman E, Hu L. *Angew Chem Int Ed*, 2017, 56: 14942–14947
57 Shao Y, Wang H, Gong Z, Wang D, Zheng B, Zhu J, Lu Y, Hu YS, Guo X, Li H, Huang X, Yang Y, Nan CW, Chen L. *ACS Energy Lett*, 2018, 3: 1212–1218
58 Wang C, Gong Y, Liu B, Fu K, Yao Y, Hitz E, Li Y, Dai J, Xu S, Luo W, Wachsman ED, Hu L. *Nano Lett*, 2017, 17: 565–571
59 Shi K, Wan Z, Yang L, Zhang Y, Huang Y, Su S, Xia H, Jiang K, Shen L, Hu Y, Zhang S, Yu J, Ren F, He YB, Kang F. *Angew Chem Int Ed*, 2020, 59: 11784–11788
60 Wu W, Duan J, Wen J, Chen Y, Liu X, Huang L, Wang Z, Deng S, Huang Y, Luo W. *Sci China Chem*, 2020, 63: 1483–1489
61 Xu P, Rheinheimer W, Shuvo SN, Qi Z, Levit O, Wang H, Ein-Eli Y, Stanciu LA. *ChemElectroChem*, 2019, 6: 4576–4585
62 Zhu Y, He X, Mo Y. *J Mater Chem A*, 2016, 4: 3253–3266
63 Zhu Y, He X, Mo Y. *ACS Appl Mater Interfaces*, 2015, 7: 23685–23693
64 Lotsch BV, Maier J. *J Electroceram*, 2017, 38: 128–141
65 Butler KT, Sai Gautam G, Canepa P. *npj Comput Mater*, 2019, 5: 19
66 Han F, Gao T, Zhu Y, Gaskell KJ, Wang C. *Adv Mater*, 2015, 27: 3473–3483
67 Ohta S, Kobayashi T, Asaoka T. *J Power Sources*, 2011, 196: 3342–3345
68 Li Y, Zhou W, Chen X, Lü X, Cui Z, Xin S, Xue L, Jia Q, Goodenough JB. *Proc Natl Acad Sci USA*, 2016, 113: 13313–13317
69 Chung H, Kang B. *Chem Mater*, 2017, 29: 8611–8619
70 Wenzel S, Randau S, Leichtweiß T, Weber DA, Sann J, Zeier WG, Janek J. *Chem Mater*, 2016, 28: 2400–2407
71 Wenzel S, Leichtweiss T, Krüger D, Sann J, Janek J. *Solid State Ion*, 2015, 278: 98–105
72 Sakuda A, Hayashi A, Tatsumisago M. *Chem Mater*, 2010, 22: 949–956
73 Haruyama J, Sodeyama K, Tateyama Y. *ACS Appl Mater Interfaces*, 2017, 9: 286–292
74 Woo JH, Trevey JE, Cavanagh AS, Choi YS, Kim SC, George SM, Oh KH, Lee SH. *J Electrochem Soc*, 2012, 159: A1120–A1124
75 Park K, Yu BC, Jung JW, Li Y, Zhou W, Gao H, Son S, Goodenough JB. *Chem Mater*, 2016, 28: 8051–8059
76 Song YX, Shi Y, Wan J, Lang SY, Hu XC, Yan HJ, Liu B, Guo YG, Wen R, Wan LJ. *Energy Environ Sci*, 2019, 12: 2496–2506
77 Kitaura H, Hayashi A, Tadanaga K, Tatsumisago M. *J Power Sources*, 2009, 189: 145–148
78 Liang J, Li X, Zhao Y, Goncharova LV, Li W, Adair KR, Banis MN, Hu Y, Sham T-, Huang H, Zhang L, Zhao S, Lu S, Li R, Sun X. *Adv Energy Mater*, 2019, 9: 1902125
79 Lee YG, Fujiki S, Jung C, Suzuki N, Yashiro N, Omoda R, Ko DS, Shiratsuchi T, Sugimoto T, Ryu S, Ku JH, Watanabe T, Park Y, Aihara Y, Im D, Han IT. *Nat Energy*, 2020, 5: 299–308
80 Nolan AM, Liu Y, Mo Y. *ACS Energy Lett*, 2019, 4: 2444–2451
81 Zhao Y, Zheng K, Sun X. *Joule*, 2018, 2: 2583–2604
82 Zhao Y, Sun X. *ACS Energy Lett*, 2018, 3: 899–914
83 Ihrig M, Finsterbusch M, Tsai CL, Laptev AM, Tu C, Bram M, Sohn YJ, Ye R, Sevinc S, Lin S, Fattakhova-Rohlfing D, Guillon O. *J Power Sources*, 2021, 482: 228905
84 Bram M, Laptev AM, Mishra TP, Nur K, Kindelmann M, Ihrig M, Pereira da Silva JG, Steinert R, Buchkremer HP, Litnovsky A, Klein

F, Gonzalez-Julian J, Guillon O. *Adv Eng Mater*, 2020, 22: 2000051
85 Yao X, Huang N, Han F, Zhang Q, Wan H, Mwizerwa JP, Wang C, Xu X. *Adv Energy Mater*, 2017, 7: 1602923
86 Duan H, Fan M, Chen WP, Li JY, Wang PF, Wang WP, Shi JL, Yin YX, Wan LJ, Guo YG. *Adv Mater*, 2019, 31: 1807789
87 Liang J, Li X, Wang S, Adair KR, Li W, Zhao Y, Wang C, Hu Y, Zhang L, Zhao S, Lu S, Huang H, Li R, Mo Y, Sun X. *J Am Chem Soc*, 2020, 142: 7012–7022
88 Li X, Liang J, Yang X, Adair KR, Wang C, Zhao F, Sun X. *Energy Environ Sci*, 2020, 13: 1429–1461
89 Zhang B, Weng M, Lin Z, Feng Y, Yang L, Wang LW, Pan F. *Small*, 2020, 16: 1906374
90 de Klerk NJJ, Wagemaker M. *ACS Appl Energy Mater*, 2018, 1: 5069–5618
91 Maier J. *Prog Solid State Chem*, 1995, 23: 171–263
92 Yamamoto K, Iriyama Y, Asaka T, Hirayama T, Fujita H, Fisher CAJ, Nonaka K, Sugita Y, Ogumi Z. *Angew Chem Int Ed*, 2010, 49: 4414–4417
93 Fingerle M, Buchheit R, Sicolo S, Albe K, Hausbrand R. *Chem Mater*, 2017, 29: 7675–7685
94 Yamamoto K, Iriyama Y, Asaka T, Hirayama T, Fujita H, Nonaka K, Miyahara K, Sugita Y, Ogumi Z. *Electrochem Commun*, 2012, 20: 113–116
95 Liang JY, Zeng XX, Zhang XD, Wang PF, Ma JY, Yin YX, Wu XW, Guo YG, Wan LJ. *J Am Chem Soc*, 2018, 140: 6767–6770
96 Ohta N, Takada K, Zhang L, Ma R, Osada M, Sasaki T. *Adv Mater*, 2006, 18: 2226–2229
97 Gittleson FS, El Gabaly F. *Nano Lett*, 2017, 17: 6974–6982
98 Gao B, Jalem R, Ma Y, Tateyama Y. *Chem Mater*, 2020, 32: 85–96
99 Wang L, Xie R, Chen B, Yu X, Ma J, Li C, Hu Z, Sun X, Xu C, Dong S, Chan TS, Luo J, Cui G, Chen L. *Nat Commun*, 2020, 11: 5889
100 Tian HK, Qi Y. *J Electrochem Soc*, 2017, 164: E3512–E3521
101 Zhao CZ, Duan H, Huang JQ, Zhang J, Zhang Q, Guo YG, Wan LJ. *Sci China Chem*, 2019, 62: 1286–1299
102 Xie H, Hao Q, Jin H, Xie S, Sun Z, Ye Y, Zhang C, Wang D, Ji H, Wan LJ. *Sci China Chem*, 2020, 63: 1306–1314
103 Kasemchainan J, Zekoll S, Spencer Jolly D, Ning Z, Hartley GO, Marrow J, Bruce PG. *Nat Mater*, 2019, 18: 1105–1111
104 Huo H, Chen Y, Zhao N, Lin X, Luo J, Yang X, Liu Y, Guo X, Sun X. *Nano Energy*, 2019, 61: 119–125
105 Li Y, Chen X, Dolocan A, Cui Z, Xin S, Xue L, Xu H, Park K, Goodenough JB. *J Am Chem Soc*, 2018, 140: 6448–6455
106 Doux J-, Nguyen H, Tan DHS, Banerjee A, Wang X, Wu EA, Jo C, Yang H, Meng YS. *Adv Energy Mater*, 2020, 10: 1903253
107 Krauskopf T, Mogwitz B, Rosenbach C, Zeier WG, Janek J. *Adv Energy Mater*, 2019, 9: 1902568
108 Liu L, Qi X, Ma Q, Rong X, Hu YS, Zhou Z, Li H, Huang X, Chen L. *ACS Appl Mater Interfaces*, 2016, 8: 32631–32636
109 Groh MF, Sullivan MJ, Gaultois MW, Pecher O, Griffith KJ, Grey CP. *Chem Mater*, 2018, 30: 5886–5895
110 Ohta S, Komagata S, Seki J, Saeki T, Morishita S, Asaoka T. *J Power Sources*, 2013, 238: 53–56
111 Liu T, Ren Y, Shen Y, Zhao SX, Lin Y, Nan CW. *J Power Sources*, 2016, 324: 349–357
112 Dong D, Zhou B, Sun Y, Zhang H, Zhong G, Dong Q, Fu F, Qian H, Lin Z, Lu D, Shen Y, Wu J, Chen L, Chen H. *Nano Lett*, 2019, 19: 2343–2349
113 Liang JY, Zeng XX, Zhang XD, Zuo TT, Yan M, Yin YX, Shi JL, Wu XW, Guo YG, Wan LJ. *J Am Chem Soc*, 2019, 141: 9165–9169
114 van den Broek J, Afyon S, Rupp JLM. *Adv Energy Mater*, 2016, 6: 1600736
115 Hitz GT, McOwen DW, Zhang L, Ma Z, Fu Z, Wen Y, Gong Y, Dai J, Hamann TR, Hu L, Wachsman ED. *Mater Today*, 2019, 22: 50–57
116 Jin Y, Liu K, Lang J, Zhuo D, Huang Z, Wang C, Wu H, Cui Y. *Nat Energy*, 2018, 3: 732–738
117 Jin Y, Liu K, Lang J, Jiang X, Zheng Z, Su Q, Huang Z, Long Y, Wang C, Wu H, Cui Y. *Joule*, 2020, 4: 262–274
118 Lu Y, Chen J. *Nat Rev Chem*, 2020, 4: 127–142
119 Strauss F, Bartsch T, de Biasi L, Kim AY, Janek J, Hartmann P, Brezesinski T. *ACS Energy Lett*, 2018, 3: 992–996
120 Koerver R, Aygün I, Leichtweiß T, Dietrich C, Zhang W, Binder JO, Hartmann P, Zeier WG, Janek J. *Chem Mater*, 2017, 29: 5574–5582
121 Xu Z, Rahman MM, Mu L, Liu Y, Lin F. *J Mater Chem A*, 2018, 6: 21859–21884
122 Ruess R, Schweidler S, Hemmelmann H, Conforto G, Bielefeld A, Weber DA, Sann J, Elm MT, Janek J. *J Electrochem Soc*, 2020, 167: 100532
123 Bucci G, Talamini B, Renuka Balakrishna A, Chiang YM, Carter WC. *Phys Rev Mater*, 2018, 2: 105407
124 Zhang W, Schröder D, Arlt T, Manke I, Koerver R, Pinedo R, Weber DA, Sann J, Zeier WG, Janek J. *J Mater Chem A*, 2017, 5: 9929–9936
125 de Biasi L, Lieser G, Dräger C, Indris S, Rana J, Schumacher G, Mönig R, Ehrenberg H, Binder JR, Geßwein H. *J Power Sources*, 2017, 362: 192–201
126 Ariyoshi K, Yamamoto H, Yamada Y. *Electrochim Acta*, 2018, 260: 498–503
127 Ariyoshi K, Orikasa Y, Kajikawa K, Yamada Y. *J Mater Chem A*, 2019, 7: 13641–13649
128 Strauss F, de Biasi L, Kim AY, Hertle J, Schweidler S, Janek J, Hartmann P, Brezesinski T. *ACS Mater Lett*, 2020, 2: 84–88
129 Besli MM, Xia S, Kuppan S, Huang Y, Metzger M, Shukla AK, Schneider G, Hellstrom S, Christensen J, Doeff MM, Liu Y. *Chem Mater*, 2019, 31: 491–501
130 Lewis JA, Cortes FJQ, Liu Y, Miers JC, Verma A, Vishnugopi BS, Tippens J, Prakash D, Marchese TS, Han SY, Lee C, Shetty PP, Lee HW, Shevchenko P, De Carlo F, Saldana C, Mukherjee PP, McDowell MT. *Nat Mater*, 2021, doi: 10.1038/s41563-020-00903-2
131 Zhang C, Feng Y, Han Z, Gao S, Wang M, Wang P. *Adv Mater*, 2019, 32: 1903747
132 Zhang C, Firestein KL, Fernando JFS, Siriwardena D, von Treifeldt JE, Golberg D. *Adv Mater*, 2020, 32: 1904094
133 Cao C, Toney MF, Sham TK, Harder R, Shearing PR, Xiao X, Wang J. *Mater Today*, 2020, 34: 132–147
134 Xiang Y, Li X, Cheng Y, Sun X, Yang Y. *Mater Today*, 2020, 36: 139–157